THE FASEB JOURNAL • RESEARCH • www.fasebj.org

Endoglin interacts with VEGFR2 to promote angiogenesis

Hongyu Tian,[*,1] Jennifer J. Huang,[†] Christelle Golzio,[‡] Xia Gao,[§] Melissa Hector-Greene,[†] Nicholas Katsanis,[‡] and Gerard C. Blobe[*,†,2]

[*]Division of Medical Oncology, Department of Medicine, [†]Department of Pharmacology and Cancer Biology, [‡]Center for Human Disease Modeling, Duke University Medical Center, and [§]Department of Cell Biology, School of Medicine, Duke University, Durham, North Carolina, USA

ABSTRACT: Endoglin, a TGF-β coreceptor predominantly expressed in endothelial cells, plays an important role in vascular development and tumor-associated angiogenesis. However, the mechanism by which endoglin regulates angiogenesis, especially during tip cell formation, remains largely unknown. In this study, we report that endoglin promoted VEGF-induced tip cell formation. Mechanistically, endoglin interacted with VEGF receptor (VEGFR)-2 in a VEGF-dependent manner, which sustained VEGFR2 on the cell surface and prevented its degradation. Endoglin mutants deficient in the ability to interact with VEGFR2 failed to sustain VEGFR2 on the cell surface and to promote VEGF-induced tip cell formation. Further, an endoglin-targeting monoclonal antibody (mAb), TRC105, cooperated with a VEGF-A targeting mAb, bevacizumab, to inhibit VEGF signaling and tip cell formation *in vitro* and to inhibit tumor growth, metastasis, and tumor-associated angiogenesis in a murine tumor model. This study demonstrate a novel mechanism by which endoglin initiates and regulates VEGF-driven angiogenesis while providing a rationale for combining anti-VEGF and anti-endoglin therapy in patients with cancer.—Tian, H., Huang, J. J., Golzio, C., Gao, X., Hector-Greene, M., Katsanis, N., Blobe, G. C. Endoglin interacts with VEGFR2 to promote angiogenesis. FASEB J. 32, 000–000 (2018). www.fasebj.org

KEY WORDS: endothelial · sprouting · VEGF · signaling · cancer

Angiogenesis is the physiologic process by which new blood vessels arise from pre-existing vessels. It has prominent roles in both physiologic processes (*i.e.*, embryonic development and wound healing) and pathologic conditions, including cancer. The growth of a primary tumor beyond 1–2 mm^3 depends on the oxygen, nutrients, and growth factors supplied *via* tumor-associated angiogenesis. In addition, tumor-associated blood vessels provide primary cancer cells a route for dissemination to distant organs. Angiogenesis is a complicated process that is tightly regulated by several angiogenic and antiangiogenic factors, including VEGF, fibroblast growth factor, and the TGF-β superfamily.

VEGFs are a family of heparin-binding growth factors, consisting of 5 members: VEGF-A, -B, -C, and -D and placental growth factor. Among them, VEGF-A and its primary receptor, VEGF receptor (VEGFR)-2, have a key role in most phases of angiogenesis (1). Upon VEGF-A stimulation, a subgroup of endothelial cells is selected to form tip cells, which initialize sprouting of a nascent blood vessel. Endothelial tip cells remain at the growing end of a nascent vascular sprout and are characterized by abundant and dynamic filopodia. VEGFR2, which is highly expressed on tip cells relative to stalk and phalanx endothelial cells, allows these tip cells to extend filopodia and detect the VEGF-A gradient to promote directed migration along this gradient (2). VEGF-A also induces expression of delta-like ligand-4, a ligand for the Notch pathway, specifically in tip cells. The binding of delta-like ligand-4 with Notch receptors expressed in neighboring cells suppresses the tip phenotype in adjacent (stalk) endothelial cells (3, 4).

The TGF-β superfamily has central roles in regulating developmental and tumor-associated angiogenesis (5, 6). The canonical TGF-β superfamily signaling pathway is triggered when TGF-β superfamily ligands bind to cell surface receptors, including

ABBREVIATIONS: ALK, activin receptor-like kinase; BMP, bone morphogenetic protein; DLAV, dorsal longitudinal anastomotic vessels; EGFP, enhanced GFP; *ENG*, endoglin (gene); EV, empty vector; FBS, fetal bovine serum; GFP, green fluorescent protein; HA, human influenza hemagglutinin; HHT, hereditary hemorrhagic helangiectasia; HMEC, human microvascular endothelial cell; hpf, hours post-fertilization; IP, immunoprecipitation, immunoprecipitate; ISV, intersegmental vessels; mAb, monoclonal antibody; MEEC, mouse embryonic endothelial cells; MO, morpholino; NAAIRS, asparagine-alanine-alanine-isoleucine-arginine-serine; NTC, nontargeted control; PLA, proximity ligation assay; sh, short hairpin; Smad, mothers against decapentaplegic; TβRI, TGF-β receptor (types I–III); VEGFR2, VEGF receptor 2; WT, wild type

[1] Correspondence: Department of Medicine, Duke University Medical Center, B354 LSRC, Box 91004 DUMC, Research Dr., Durham, NC 27708, USA. E-mail: hongyu.tian@duke.edu

[2] Correspondence: Department of Medicine, Duke University Medical Center, B354 LSRC, Box 91004 DUMC, Research Dr., Durham, NC 27708, USA. E-mail: gerard.blobe@duke.edu

doi: 10.1096/fj.201700867RR

This article includes supplemental data. Please visit *http://www.fasebj.org* to obtain this information.

coreceptors [TGFβ receptor (TβR)-II and endoglin], type II (TβRII), and type I (TβRI). Upon ligand binding, these receptors form complexes to transphosphorylate and activate TβRI by TβRII. TβRI then phosphorylates receptor-regulated small mothers against decapentaplegic (R-Smads), which form a Smad complex by binding the co-Smad (Smad4), and then translocate to the nucleus to regulate target gene expression by acting in concert with coactivators and corepressors (7). Endothelial cells express 2 type I TGF-β superfamily receptors: activin-like kinase-1 (ALK1, expressed preferentially in the endothelium) and ALK5 (expressed ubiquitously) (8, 9), which activate the Smad1/5/8 pathway and Smad2/3 pathway, respectively. The balance of ALK1/Smad1/5/8 and ALK5/Smad2/3 determines the TGF-β superfamily's responsiveness in endothelial cell biology (8, 9). Recent studies have demonstrated that bone morphogenetic protein (BMP)-9, another TGF-β superfamily ligand, also binds to ALK1 and endoglin with high affinity to activate Smad1/5/8 pathway (10) and controls quiescence in adult blood vessels (11).

Among TGF-β receptors, ALK1 and its coreceptor, endoglin, are expressed preferentially in endothelial cells. Mice null for ALK1 or endoglin experience embryonic lethality caused by defects in vascular development at days 10–11.5 (12, 13). In humans, mutations in endoglin and ALK1 result in hereditary hemorrhagic telangiectasia (HHT), an autosomal dominant vascular disease characterized by arteriovenous malformations and dilated vessels that lead to recurrent hemorrhage and shunting in the brain, gastrointestinal tract, and lung (14, 15). In addition, endoglin is overexpressed in neoangiogenic vessels and in solid tumors (16). Tumor-associated angiogenesis is generally triggered by angiogenic factors, including VEGF, induced by hypoxic conditions (17). Endoglin expression is also upregulated under hypoxic conditions (18, 19). These findings suggest that endoglin cooperates with VEGF to promote tumor-associated angiogenesis. Recent reports demonstrate that endoglin can promote tip cell formation and that it modulates VEGFR2 signaling but that it may not be required for angiogenesis (20–22). However, how endoglin regulates tip cell formation and the mechanism by which endoglin regulates the VEGF or Notch signaling pathways remains unknown. We investigated the role and mechanism of endoglin in regulating VEGF signaling and VEGF-mediated sprouting and angiogenesis.

MATERIALS AND METHODS

Cell culture and reagents

Human microvascular endothelial cells (HMEC)-1s were obtained from Dr. Edwin Ades (Centers for Disease Control, Atlanta, GA, USA). HMEC-1s were grown in MCDB-131 medium (Millipore-Sigma, Billerica, MA, USA), supplemented with 10% fetal bovine serum (FBS; Corning, Corning, NY, USA), 10 ng/ml EGF (Millipore-Sigma), 1 μg/ml hydrocortisone (Millipore-Sigma), and 2 mM L-glutamine (Thermo Fisher Scientific, Waltham, MA, USA). Mouse embryonic endothelial cells (MEECs) (23) were obtained from Dr. Elisabetta Dejana (University of Milan, Milan, Italy). MEECs were grown in MCDB-131 medium supplemented with 10% fetal bovine serum (FBS), 1 mM sodium pyruvate (Thermo Fisher Scientific), 2 mM L-glutamine (Thermo Fisher Scientific), 100 μg heparin (Millipore-Sigma), and 50 μg/ml endothelial cell growth supplement (Millipore-Sigma). The 4T1 cells stably expressing the firefly luciferase gene (under the selection of puromycin) were obtained from Dr. Mark W. Dewhirst (Duke University Medical Center). 4T1 cells were grown in DMEM (Thermo Fisher Scientific), supplemented with 10% FBS. COS7 cells (purchased from American Type Culture Collection, Manassas, VA, USA) were grown in DMEM, supplemented with 10% FBS. Human mammary epithelial cells (HMEC)-1s were authenticated, and all cells were tested for mycoplasma contamination. Endoglin antibody [catalog number (P3D1)] was purchased from Developmental Studies Hybridoma Bank (University of Iowa, Iowa City, IA, USA). Phospho-VEGFR2 (Tyr1175, 2478; Tyr949, 4991; and Tyr1212: 2477), VEGFR2 (9698), phospho-Erk1/2 (9101), ERK1/2 (9102), Smad1 (9743), phosphor-Smad1/5/8 (9511), Smad1 (9743), phosphor-Smad2 (3101), Smad2 (3103), antibodies were all purchased from Cell Signaling Technology (Danvers, MA, USA). CD31 antibody (ab28364) antibody was purchased from Abcam, Inc. (Cambridge, United Kingdom). HA-antibody (1-666-606) was purchased from Roche (Basel, Switzerland). Streptavidin, horseradish peroxidase conjugate (OR03L) was purchased from Millipore-Sigma.

Protein overexpression and knockdown

MEECs and COS7 cells were transfected with Lipofectamine 2000 transfection reagent (Thermo Fisher Scientific) (24–26). HMEC-1s were infected with either a nontargeting vector control (NTC) or shRNA endoglin-expressing pGIPZ lentivirus (target sequence: 5′-GCCATGACCCTGGTACTAA-3′, RHS4430-99141476; GE Healthcare, Chicago, IL, USA), and stably infected cells were selected for 72 h with 1 μg/ml puromycin.

Spheroid-based sprouting assay

HMEC-1 or MEEC spheroids were prepared as reported (25, 27). In brief, 1×10^3 HMEC-1s or MEECs were cultured in hanging drops of 25 μl medium (80% regular medium and 20% Methocel; Dow Chemical Co., Midland, MI, USA) and allowed to aggregate as spheroids for 24 h. The spheroids were then collected and plated on 24-well plates coated with growth factor–reduced Matrigel (BD Biosciences, San Jose, CA, USA) and treated. Sprouts were digitally imaged and the number and length of sprouts per spheroid were quantified with ImageJ software (National Institutes of Health, Bethesda, MD, USA). For the tip cell competition assay, MEECs$^{+/+}$ or wild-type (WT) were labeled with the PKH26 Red Fluorescent Cell Linker Mini Kit (Millipore-Sigma), MEECs$^{-/-}$ were stained with the PKH67 Green Fluorescent Cell Linker Mini Kit (Millipore-Sigma). Stained MEECs$^{+/+}$ and MEECs$^{-/-}$ or stained WT HMEC-1s and short hairpin (sh)*ENG* HMEC-1s [with green fluorescent protein (GFP)] were mixed at a 1:1 ratio. Mixed endothelial cells (1×10^3) were cultured in hanging drops to make spheroids, and the sprouting assay was performed. Sprouts were digitally imaged with a fluorescence microscope and quantified.

Western blot analysis

MEECs or HMEC-1s were serum starved for 6 h and treated with 50 ng/ml VEGF-A (293-VE-010; R&D Systems,

Minneapolis, MN, USA) for 5 min, or 50 pM TGF-1 (240-B; R&D Systems), or with 2 ng/ml BMP-9 (3209-BP-010; R&D Systems) for 30 min. Cells were then lysed using 2× sample buffer and subjected to Western blot analysis as previously described (24–26). The bands on Western blots were quantified for integrated density using ImageJ.

Coimmunoprecipitation

MEECs$^{+/+}$, MEECs$^{-/-}$ or COS7 cells coexpressing human influenza hemagglutinin (HA)–tagged endoglin (HA-endoglin) and VEGFR2 for 24 h were washed with PBS and then lysed on ice with lysis buffer containing 137 mM NaCl, 20 mM Tris-HCl (pH 8.0), 10 mM NaF, 2 mM EDTA, 1% NP-40, 10% glycerol, 1 mM PMSF, 5 μg/ml leupeptin, and 1 mM Na_3VO_4. The lysates were incubated with anti-HA, P3D1, or VEGFR2 antibodies at 4°C overnight, followed by incubation with protein G-agarose beads (for anti-HA and P3D1; GE Healthcare) or protein A-agarose beads (for anti-VEGFR2; GE Healthcare) for 1 h. The immunoprecipitate (IP) was collected by centrifugation, and the pellets were washed with lysis buffer and boiled in 2× sample buffer at 100°C for 10 min before Western blot analysis.

Protein detection assay

A protein detection assay (Duolink; Millipore-Sigma) was performed according to the manufacturer's protocol. In brief, MEECs$^{+/+}$ were serum starved for 6 h before treatment with 50 ng/ml VEGF-A for 5, 10, and 15 min. Cells were then fixed with 4% paraformaldehyde, permeabilized in PBS containing 0.1% Triton X-100 for 5 min, and blocked with 3% BSA (in PBS) for 1 h. Slides were incubated with P3D1 and anti-VEGFR2 primary antibodies for 1 h at room temperature and then incubated with proximity ligation assay (PLA) probe, without and with mixture for 1 h at 37°C. After ligation for 30 min and amplification for 100 min at 37°C, slides were labeled with DAPI and mounted in Prolong Anti-Fade medium (Millipore-Sigma). The slides were digitally imaged, and the number of red dots per cell were counted using ImageJ software. For each condition, ~100 cells were quantified.

Morpholino and embryo manipulations

Endoglin splice blocker morpholinos (MOs) (5′-TAGTAGAGAACTTACCCGCACAGGC-3′) were obtained from Gene Tools, LLC (Philomath, OR, USA). RT-PCR was performed to determine endoglin MO efficacy with gene-specific primers in exons immediately flanking the targeted region on 72 h postfertilization (hpf) RNA isolated from control and Endo MO-injected embryos. One nanoliter of diluted MO (8 ng), with or without RNA (100 pg), was injected into transgenic [*Fli1*:enhanced green fluorescent protein (*EGFP*)] zebrafish embryos at the 1–2-cell stage. Injected embryos were raised with 0.2 mM 1-phenyl-2-thio-urea (Millipore-Sigma) at 24 hpf, to prevent pigment formation, and were allowed to develop until 48 hpf. Injected embryos were scored at 48 hpf and classified into 3 groups: normal; class I (mild, with 1–3 intersegmental vessels affected); and class II (severe, with 3+ intersegmental vessels affected). They were then compared to age-matched controls from the same clutch. For RNA rescue experiments, human endoglin mRNAs, WT, and mutants N3and N6 were transcribed *in vitro* with the SP6 Message Machine Kit (Thermo Fisher Scientific). A χ^2 test was performed from 3 independent experiments to determine the significance of phenotypic rescue.

Trypsin internalization assay

MEECs$^{+/+}$, and MEECs$^{-/-}$, or MEECs$^{-/-}$ overexpressing empty vector (EV) or HA-endoglin were incubated with 0.5 mg/ml sulfo-NHS-LC-biotin (Thermo Fisher Scientific) in 4-(2-hydroxyethyl)-1-piperazineethanesulfonic acid (HEPES) buffer, containing (mM) 5 KCl, 150 NaCl, 1.2 $MgCl_2$, 1.3 $CaCl_2$, and 10 HEPES, at 4°C for 2 h. Cells were rinsed twice with ice-cold PBS. The cells were treated with 1 ml prewarmed MEEC medium, containing 50 ng/ml VEGF-A and incubated for a time course at 37°C that promoted internalization of cell surface proteins. Cells were then washed once with PBS on ice, incubated with trypsin at 37°C for 1 min, and immediately added to MEEC medium on ice. Cells were collected and lysed on ice with 1 ml RIPA with protease inhibitors (pepstatin, leupeptin, and PMSF) and centrifuged at 14,000 rpm for 30 min at 4°C. Pellets were removed, the supernatants were immunoprecipitated with anti-VEGFR2 antibody and resolved by SDS-PAGE, and the internalized biotinylated VEGFR2 was blotted with streptavidin-horseradish peroxidase.

In vivo tumorigenicity and metastasis assay

4T1 cells were implanted into the inguinal mammary fat pads of 25 6-wk-old female BALB/c mice (5×10^4 cells/mouse). Cohorts were randomly divided into 4 groups 7 d after injection: untreated ($n = 7$) and mice treated with B20-4.1 ($n = 6$) (Genentech, San Francisco, CA, USA), TRC105 ($n = 6$) (Tracon Pharma, San Diego, CA, USA), or both ($n = 6$). The mice were treated with 5 mg/kg B20-4.1, with or without 15 mg/kg TRC105 twice per week *via* intraperitoneal injection. Tumor size was measured by researchers blinded to treatment condition, and tumor size calculated was $1/2 \times (\text{length} \times \text{width}^2)$. Among all the mice, 1 mouse in the combination treatment group died accidentally, and the data acquired from this mouse was excluded. Tumor metastasis was monitored once per week *via* bioluminescence imaging. All the mice were euthanized after 3 wk of treatment. All procedures and animal studies were approved by Duke University's Institutional Animal Care and Use Committee.

CD31 immunofluorescent staining

The primary tumor tissues were fixed in 4% paraformaldehyde at 4°C overnight. Samples were embedded in paraffin and sliced into 7 μm sections. After deparaffinization and rehydration, the sections were subjected to antigen retrieval in 10 mM sodium citrate (pH 6.0), with a 2100 Retriever (PickCell Laboratories, Amsterdam, The Netherlands). The tissue was quenched with 0.6% H_2O_2 (in methanol) for 15 min at room temperature and then blocked with TNT blocking buffer, containing 0.15 M NaCl, 0.1 M Tris-HCl (pH 7.5), and 0.5% blocking reagent. The sections were incubated with CD31 antibody (1:50 dilution) in blocking buffer at 4°C overnight. After the sections were washed, they were incubated with Peroxidase AffiniPure donkey anti-rabbit IgG (1:1000 dilution; Jackson ImmuoResearch, Philadelphia, PA, USA) for 2 h. The signal was amplified with a Tyramide Signal Amplification Plus Cyanine 3 Kit (PerkinElmer Life Sciences, Emeryville, CA, USA) according to the manufacturer's instructions. The sections were counterstained with DAPI and mounted with FluroSave reagent (Calbiochem, San Diego, CA, USA). The total area of blood vessels occupied in each field (represented as the surface density of vessels) was measured with ImageJ software.

Statistics

All experiments were repeated at least 3× with similar results each time. Statistical analysis was conducted using 1- or 2-way

ANOVA for the interaction assay, or unpaired, 2-tailed Student's t test. Statistical significance was set at $P < 0.05$. Group size was selected based on cell, reagent, or animal limitations while still achieving statistically relevant results. No data were excluded from any analyses, and all replicates are true biologic replicates. The statistical test used and the sample sizes for individual analyses are provided within the figure legends. For ANOVA tests, all P values were adjusted by not assuming equality of variances.

RESULTS

Endoglin promotes VEGF-A–induced tip cell formation and angiogenesis

To investigate endoglin's role in sprouting during angiogenesis, we assessed the effects of endoglin on VEGF-A–induced spheroid sprouting. VEGF-A induced more sprouting in endoglin-expressing human microvascular endothelial cells (HMEC-1-shNTCs; **Fig. 1*A–C***) and murine embryonic endothelial cell lines derived from WT embryos (23) (MEECs$^{+/+}$; Fig. 1*D, E*) than in HMEC-1s with stable shRNA-mediated silencing of endoglin expression (HMEC-1-sh*ENG*), Fig. 1*A*–C and Supplemental Fig. 1*A*) or MEECs from endoglin-null embryos (23) (MEECs$^{-/-}$, Fig. 1*D, E* and Supplemental Fig. 1*B*). Further, VEGF-A increased directional persistence of MEEC$^{+/+}$ cells, whereas VEGF-A–stimulated MEECs$^{-/-}$ demonstrated less directional persistence in the spheroid-based sprouting model (Fig. 1*F*).

We then labeled MEECs$^{+/+}$ or WT HMEC-1s with red fluorescence and MEECs$^{-/-}$ or HMEC-1-sh*ENG*s with green fluorescence and compared their relative occupancy of the tip cell position. HMEC-1-WT cells and MEECs$^{+/+}$ occupied the tip cell position more frequently than HMEC-1-sh*ENG* cells and MEECs$^{-/-}$ in

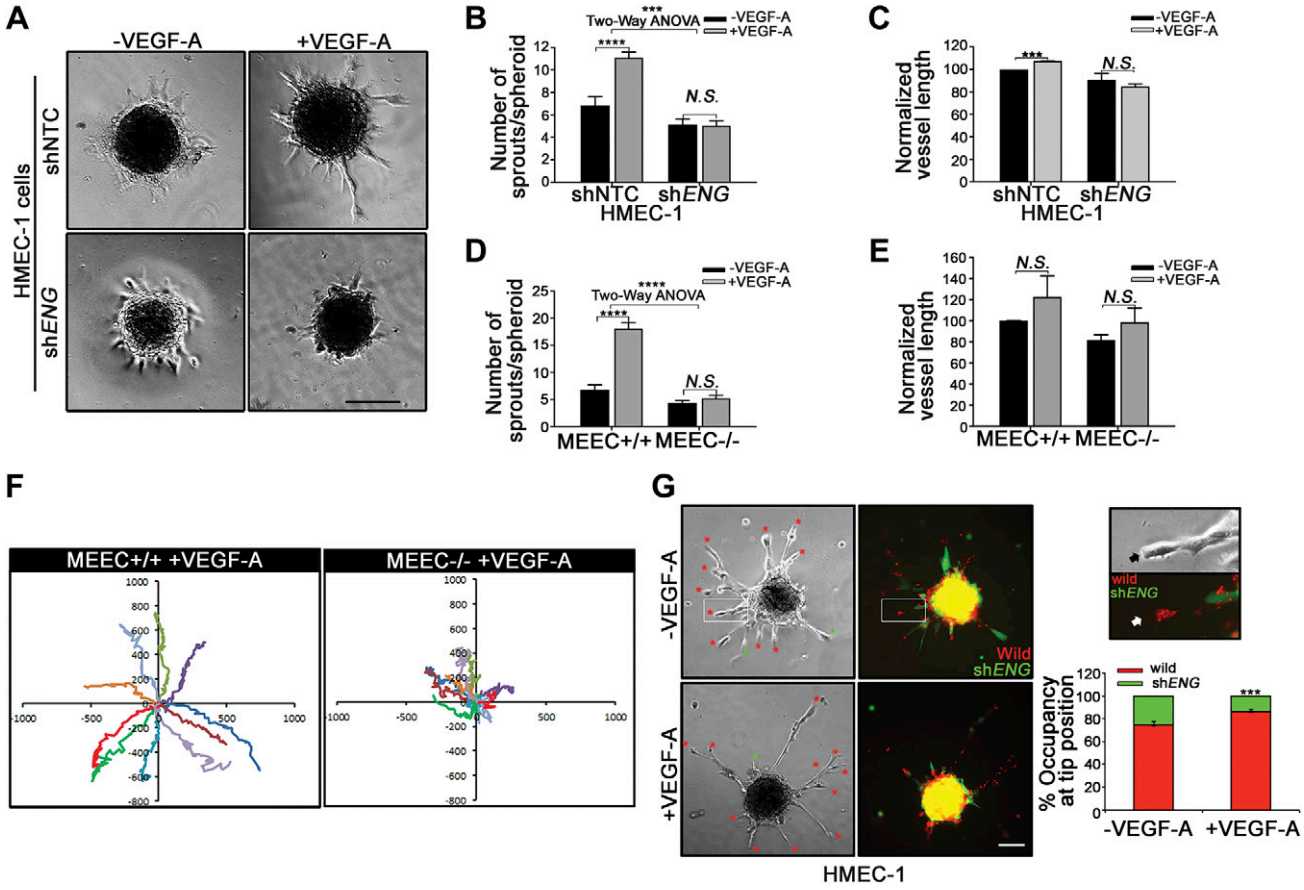

Figure 1. Endoglin promotes VEGF-induced sprouting and angiogenesis. *A–E*) Endothelial spheroids made from HMEC-1-shNTCs and -shENGs (*A–C*), or from MEECs$^{+/+}$ and MEECs$^{-/-}$ (*D, E*), were treated with or without 100 ng/ml VEGF-A and cultured on Matrigel for 18 h. The number of sprouts (*B, D*) and the length of vessels (*C, E*) were quantified by image analysis software. The length of each sprout was taken into account. The length of all the sprouts of the control cells (HMEC-1-shNTCs and MEECs$^{+/+}$) without treatment in the same batch of experiments were averaged and normalized to 100, and the relative sprouting and vessel length of other conditions were calculated relative to this value. Data are means ± SEM calculated from 3 independent experiments. ***$P < 0.001$, ****$P < 0.0001$ (2-tailed Student t test, and the statistical interaction between endoglin expression and VEGF-A treatment was obtained by 2-way ANOVA). NS, not significant. Scale bar, 300 μm. *F*) The migration path of the frontier endothelial cells during spheroid-based sprouting in MEECs$^{+/+}$ and MEECs$^{-/-}$ was captured with live cell imaging over 12 h. *G*) WT HMEC-1s were labeled with red fluorescence, mixed with HMEC-1-sh*ENG* expressing GFP at a 1:1 ratio and cultured in hanging drops to form spheroids for 24 h. The spheroids were treated, with or without 100 ng/ml VEGF-A, and cultured on the Matrigel for 18 h. The cells with red or green fluorescent protein that occupied the tip cell position were quantified from 3 experiments ± SEM. Scale bar, 100 μm. ***$P < 0.001$.

the absence of VEGF-A, and VEGF-A increased the frequency of HMEC-1-WT and MEEC$^{+/+}$ occupancy at the tip position (Fig. 1*G* and Supplemental Fig. 1*C*, *D*). The effect of endoglin was not TGF-β ligand dependent, as the pan-TGF-β neutralizing antibody, 1D11, had no effect on the tip cell occupancy frequency of MEECs$^{+/+}$ and MEECs$^{-/-}$ (Supplemental Fig. 1*D*). Consistent with a specific role for endoglin, restoring expression of endoglin in MEECs$^{-/-}$ (Supplemental Fig. 1*E*) accelerated and increased VEGF-A–induced sprouting (Supplemental Fig. 1*F*, *G*). These data indicate that endoglin has an major role in VEGF-A–induced sprouting, consistent with a recent report that endoglin can promote tip cell formation *in vivo* (20).

Endoglin promotes VEGF-A signaling

As endoglin promotes VEGF-A–induced sprouting and angiogenesis (Fig. 1) (22), we investigated whether endoglin has a role in VEGF-A signaling in endothelial cells. VEGF-A induced VEGFR2 phosphorylation (Tyr 1175) and downstream ERK1/2 phosphorylation in MEECs$^{+/+}$ (**Fig. 2*A–C***) and HMEC-1s (Supplemental Fig. 2*A*) in a time-dependent manner, with peak activation 5 min after stimulation. Loss of endoglin expression decreased VEGF-A–induced VEGFR2 phosphorylation (Tyr 1175; relative to β-actin; Fig. 2*A, B* and Supplemental Fig. 2*B*, *C*) and ERK1/2 phosphorylation (Fig. 2*C*) in MEECs$^{-/-}$ (Fig. 2*A–C*) and HMEC-1-sh*ENG* cells (Supplemental Fig. 2*B*, *C*). As VEGFR2 has multiple phosphorylation sites mediating different downstream pathways (28), we examined endoglin's role in VEGFR2 phosphorylation at different sites. Loss of endoglin decreased VEGF-A–induced VEGFR2 phosphorylation at Tyr 949, Tyr 1175, and Tyr 1212 (Supplemental Fig. 2*F*). In addition, loss of endoglin decreased basal VEGFR2 levels in MEECs (Fig. 2*A, D*) but not in HMEC-1s (Supplemental Fig. 2*B*, *D*). However, VEGF-A further decreased VEGFR2 in both MEECs$^{-/-}$ (Fig. 2*D*) and HMEC-1-sh*ENG* cells (Supplemental Fig. 2*D*) but had no effect in MEECs$^{+/+}$ and HMEC-1-shNTCs (Supplemental Fig. 2*D*). However, when p-VEGFR2 levels were normalized to total VEGFR2 levels, endoglin did not significantly alter p-VEGFR2 levels in either MEECs or HMEC-1s (Fig. 2*E* and Supplemental Fig. 2*E*), suggesting that decreased VEGF signaling in the absence of endoglin is due to decreased total VEGFR2 levels. These effects were endoglin specific, as increasing endoglin expression in MEECs$^{+/+}$ enhanced VEGF-A–induced VEGFR2 phosphorylation, while restoring endoglin expression in MEECs$^{-/-}$ rescued VEGF-A–induced VEGFR2 phosphorylation (Tyr 1175; Supplemental Fig. 2*G*).

Endoglin is a TGF-β superfamily coreceptor in endothelial cells, and mediating BMP-9 and TGF-β1 signaling (24), we investigated whether endoglin-mediated VEGF-A signaling is TGF-β ligand or receptor dependent. BMP-9 (Fig. 2*F, G*) and TGF-β1 (Supplemental Fig. 2*H–K*) increased VEGF-A induced VEGFR2 phosphorylation in both MEECs$^{+/+}$ and MEECs$^{-/-}$ (Fig. 2*F*, *G* and Supplemental Fig. 2*H*, *I*) and in HMEC-1-shNTCs and HMEC-1-sh*ENG* cells (Supplemental Fig. 2*J*, *K*). Further, even in the presence of BMP-9 (Fig. 2*F, G*) and TGF-β1 (Supplemental Fig. 2*H–K*), loss of endoglin still decreased VEGF-A–induced VEGFR2 phosphorylation. In addition, the ALK1 inhibitor ALK1-Fc (Supplemental Fig. 2*L*), the TGF-β neutralizing antibody 1D11 (Supplemental Fig. 2*M*), and the ALK5 inhibitor SB431542 did not alter the decrease in VEGF-A–induced VEGFR2 phosphorylation (Tyr 1175) induced by loss of endoglin (Fig. 2*H–K* and Supplemental Fig. 2*N*, *O*), indicating that endoglin-mediated VEGF-A signaling is not *via* TGF-β1, BMP9, ALK1, or ALK5. These data support a role for endoglin in promoting VEGF signaling through stabilizing VEGFR2 levels in endothelial cells.

Endoglin interacts with VEGFR2

To explore the mechanism by which endoglin promotes VEGF-A signaling and VEGF-A–induced angiogenesis, we investigated whether endoglin binds VEGF-A or its receptor, VEGFR2. Although VEGFR2 bound VEGF-A ligand, endoglin did not (Supplemental Fig. 3). Further, endoglin expression did not increase VEGF-A binding to VEGFR2 (Supplemental Fig. 3), suggesting that endoglin does not promote VEGF-A signaling through binding and presentation of VEGF-A ligand to VEGFR2. Because endoglin and VEGFR2 have been shown to be in proximity in endothelial cells (20), we investigated the interaction of endoglin and VEGFR2. When endoglin and VEGFR2 were coexpressed in COS7 or MEECs$^{-/-}$, endoglin coimmunoprecipitated VEGFR2 (Supplemental Fig. 4*A*, *B*). In addition, immunoprecipitation (IP) of endogenous endoglin specifically coimmunoprecipitated endogenous VEGFR2 in MEECs$^{+/+}$ but not in MEECs$^{-/-}$ (**Fig. 3*A***). In a reciprocal manner, when endoglin and VEGFR2 were coexpressed in MEECs$^{-/-}$, VEGFR2 coimmunoprecipitated endoglin (Supplemental Fig. 4*C*). Treatment with VEGF-A increased the interaction between endoglin and VEGFR2 interaction, as detected by coimmunoprecipitation (Fig. 3*B*). proximity ligation assays (PLAs) are able to detect the interaction of endogenous receptors *in situ*, and we therefore further investigated VEGF-A–induced endogenous endoglin/VEGFR2 interaction using PLAs. VEGF-A increased the interaction between endogenous endoglin and VEGFR2 (Fig. 3*C, D* and Supplemental Fig. 4*E*). Further, the VEGFR2 tyrosine kinase inhibitor, SU-5416 (29–31) (Supplemental Fig. 4*D*), decreased the VEGF-A-mediated endoglin and VEGFR2 interaction (Fig. 3*B*).

To investigate the domains of endoglin responsible for interaction with VEGFR2, we initially used endoglin truncation mutants that lack the cytoplasmic domain (ECTM) or the extracellular domain (TMCT) (Fig. 3*E*). Immunoprecipitation of WT endoglin or the TMCT mutant was able to specifically coimmunoprecipitate VEGFR2 (Fig. 3*F*). However, the endoglin ECTM mutant exhibited diminished ability to coimmunoprecipitate VEGFR2

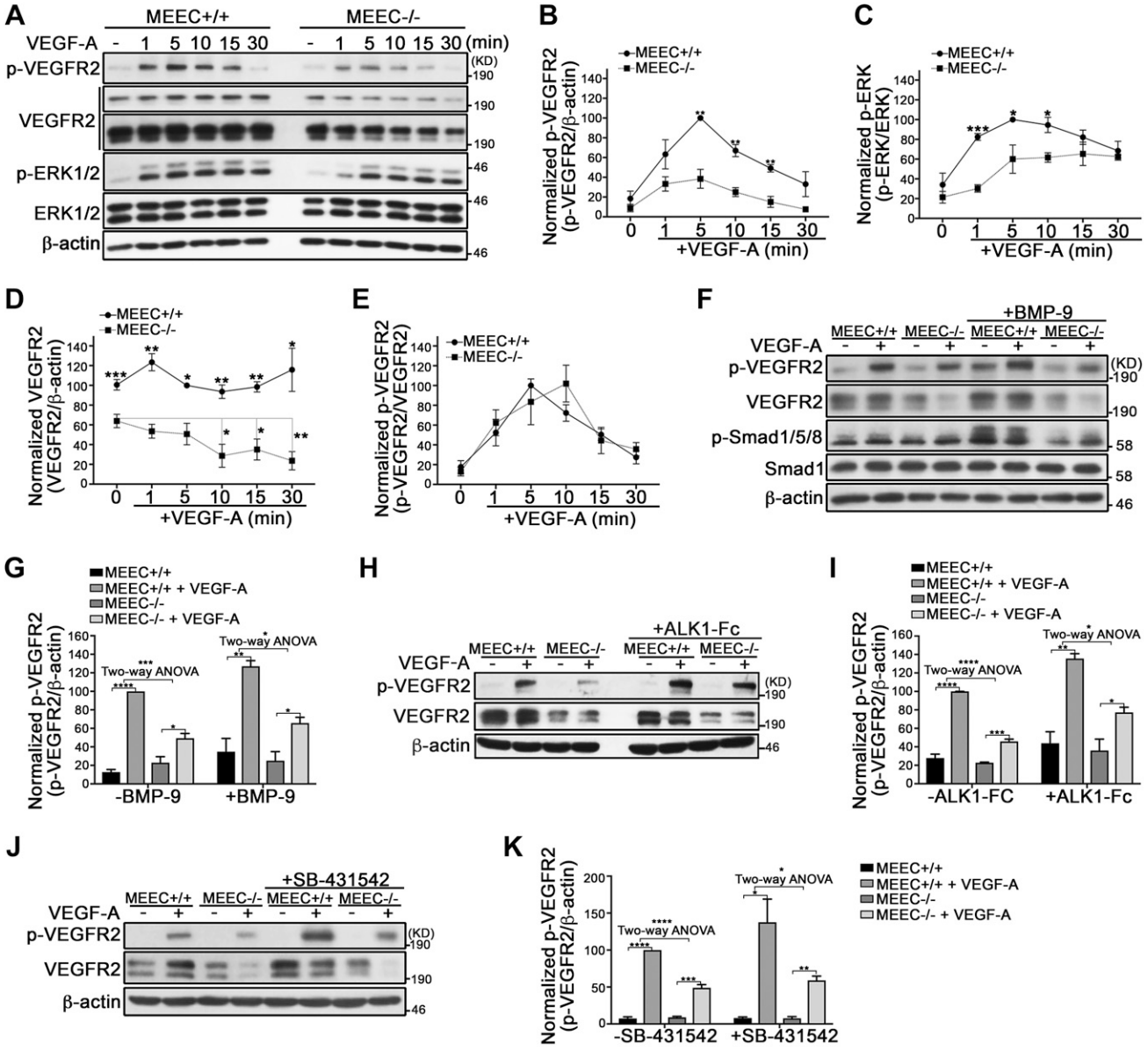

Figure 2. Endoglin promotes VEGF signaling in endothelial cells. *A–E*) MEECs$^{+/+}$ and MEECs$^{-/-}$ were serum starved for 6 h and treated with 50 ng/ml VEGF-A for the indicated times. Cell lysates were then analyzed with the indicated antibodies. The p-VEGFR2/β-actin (*B*), p-ERK/ERK (*C*), VEGFR2/β-actin (*D*), or p-VEGFR2/VEGFR2 (*E*) levels in MEECs$^{+/+}$ treated with VEGF-A for 5 min were normalized to 100, and the number of other conditions were calculated relative to this value in 3 experiments. $*P < 0.05$, $**P < 0.01$, $***P < 0.001$ (2-tailed Student's *t* test). *F–K*) MEECs$^{+/+}$ and MEECs$^{-/-}$ were serum starved for 6 h, pretreated with 5 ng/ml BMP-9 for 15 min (*F, G*), 200 ng/ml ALK1-Fc (*H, I*), or 10 μM SB-431542 (*J, K*) for 1 h and then treated with 50 ng/ml VEGF-A for 5 min; the cell lysates were analyzed with the indicated antibodies. The p-VEGFR2/β-actin levels in MEECs$^{+/+}$ treated with VEGF-A were normalized to 100, and the relative p-VEGFR2/β-actin levels of other conditions were calculated relative to this value. Quantitative data are means ± SEM from 3 independent experiments. $*P < 0.05$, $**P < 0.01$, $***P < 0.001$, $****P < 0.0001$ [2-tailed Student *t* test and the statistical interaction between BMP-9 (*G*), ALK1-Fc (*I*) or SB-431542 (*K*) treatments and endoglin expression was obtained by 2-way ANOVA].

(Fig. 3*F*), suggesting that the cytoplasmic domain of endoglin is responsible for interacting with VEGFR2. To narrow down the interaction domain in endoglin, we cotransfected MEECs$^{-/-}$ with VEGFR2 and a series of Asn-Ala-Ala-Ile-Arg-Ser (NAAIRS) mutants throughout the endoglin cytoplasmic domain (Fig. 3*E*). The NAAIRS sequence has the unique ability to adopt a variety of secondary structures depending on the surrounding native secondary structure, minimizing disruptions in overall protein structure (32). Substitution of sequences of "PVVAVA" (N3) and "SIGSTQ" (N6) with NAAIRS decreased the interaction with VEGFR2 (Fig. 3*G, H*). As there are 3 potential phosphorylation sites in the sequence ^{643}SIGSTQ$^{648,\ 643}$S, ^{646}S and ^{647}T (33), we tested whether these phosphorylation sites regulate the interaction by overexpressing endoglin serine/threonine to alanine mutants at these phosphorylation sites (Supplemental Fig. 4*F*) in MEECs$^{-/-}$. None of these phosphorylation site mutants decreased the interaction of VEGFR2 with endoglin (Supplemental Fig. 4*G*).

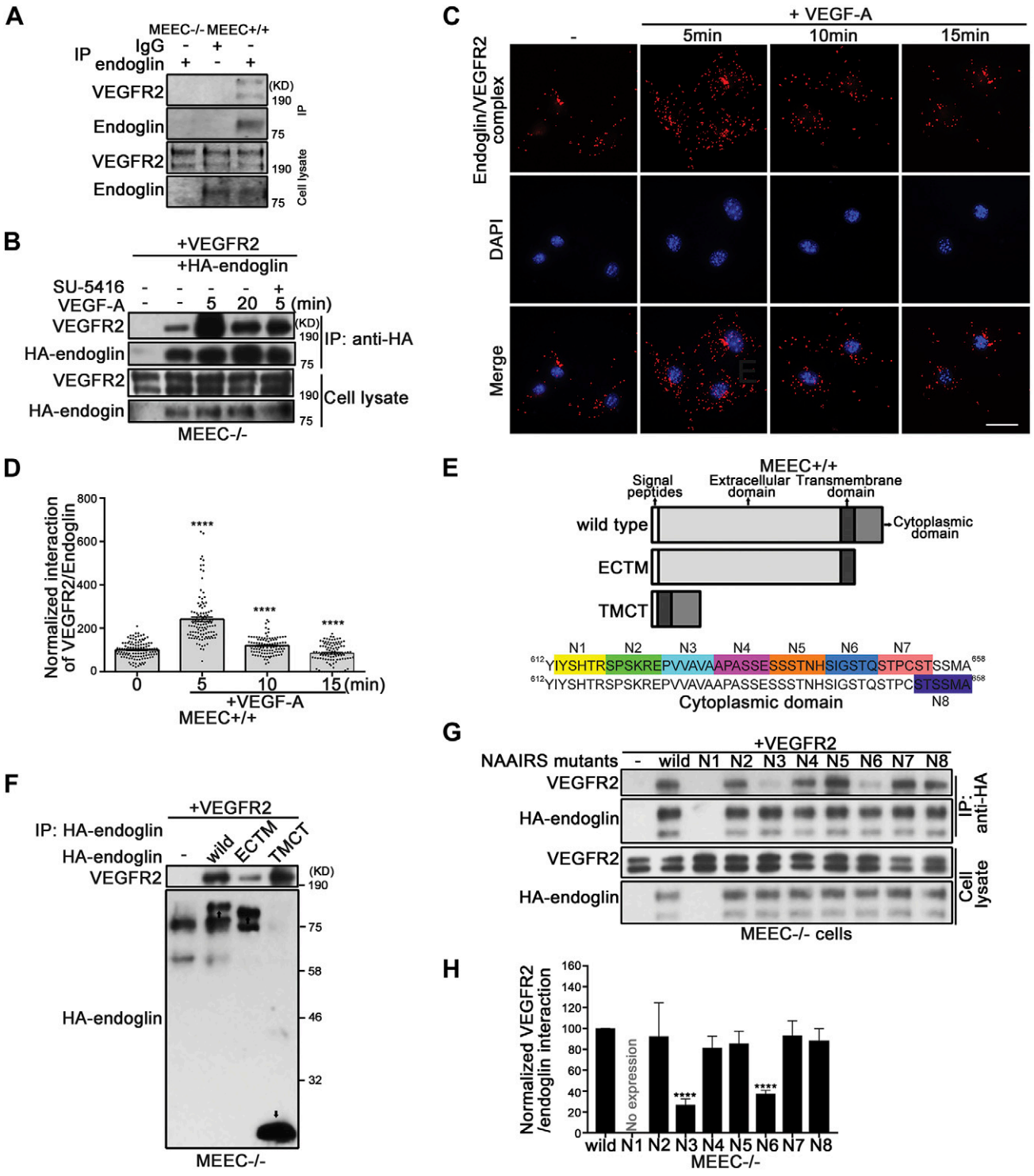

Figure 3. Endoglin interacts with VEGFR2. *A*) Immunoprecipitates were prepared from MEECs$^{+/+}$ and MEECs$^{-/-}$ with anti-endoglin antibody, P3D1, or mouse IgG. Endoglin and VEGFR2 were detected in IPs, with or without cell lysates, by Western blot analysis. Results are representative of 3 independent experiments. *B*) MEECs$^{-/-}$ were transfected with HA-endoglin and VEGFR2 for 24 h, serum starved for 6 h, pretreated with or without 1 μM SU-5416 for 1 h, and then treated with 50 ng/ml VEGF-A for the indicated times. Anti-HA IPs were prepared. HA-endoglin and VEGFR2 were detected in IP and cell lysates by Western blot analysis. Results are representative of 3 independent experiments. *C*, *D*) MEECs$^{+/+}$ were serum starved for 6 h and treated with 50 ng/ml VEGF-A for the indicated times. Interaction between endogenous endoglin and VEGFR2 was assessed by PLA. Nuclei were stained with DAPI. Each data point in *D* corresponds to the number of red dots/cell in *C*, representing the interaction between VEGFR2/endoglin. The mean value of VEGFR2/endoglin interaction in MEECs$^{+/+}$ without treatment was normalized to 100, and the relative interaction of other conditions was calculated relative to this value. NS, not significant. ****$P <$ 0.001 (2-tailed Student *t* test from 3 experiments). Scale bar, 300 μm. *E*) Schematic model of endoglin truncation or NAAIRS mutants. *F*) MEEC$^{-/-}$ were transfected with VEGFR2 and the indicated HA-endoglin truncation mutants for 24 h. Anti-HA IPs were

(*continued on next page*)

These data indicated that endoglin interact with VEGFR2 in a VEGF-A–dependent manner *via* its cytoplasmic sequences ^{625}PVVAVA^{630} and ^{643}SIGSTQ^{648}.

Endoglin and VEGFR2 interaction promotes VEGF-A–induced angiogenesis and VEGF signaling

To investigate the effects of endoglin/VEGFR2 interaction on VEGF-A signaling and biology, we transfected MEECs$^{-/-}$ with WT endoglin and N3 and N6 interaction-deficient endoglin NAAIRS mutants. Although WT endoglin rescued VEGF-A signaling, the N3 and N6 NAAIRS mutants failed to rescue VEGF-A signaling (**Fig. 4*A, B***). Moreover, the N3 and N6 NAAIRS mutants also failed to rescue VEGF-A–induced tip cell formation (Fig. 4*C, D*). To explore the physiologic relevance of our findings, we assessed the role of this endoglin function during capillary formation *in vivo* using the transgenic *Fli1-EGFP* zebrafish developmental angiogenesis model. *Fli1*-driven expression of GFP begins early in embryonic development, with angiogenesis evident within the first 24 h, as monitored *via* fluorescence microscopy. We generated morpholinos (MOs) to suppress translation of the endogenous endoglin ortholog (Endoglin-MO) in *Fli1-EGFP* embryos, and observed significant defects in the formation of both intersegmental vessels (ISVs) and dorsal longitudinal anastomotic vessel (DLAV) at 48 hpf (Fig. 4*E, F*). The injection of WT human endoglin mRNA along with Endo-MO into *Fli1-EGFP* transgenic embryos effectively rescued the phenotype (Fig. 4*F*). However, the endoglin N3 and N6 mutants, which could not interact with VEGFR2 (Fig. 3*G, H*), failed to rescue the phenotype (Fig. 4*F*), supporting a pivotal role for endoglin/VEGFR2 interaction in mediating developmental angiogenesis *in vivo*. These data indicate that endoglin and VEGFR2 interaction is necessary in both VEGF signaling and VEGF-induced tip cell formation and angiogenesis *in vitro* and *in vivo*.

Endoglin prevents VEGF-A–induced VEGFR2 internalization and degradation

As VEGF-induced receptor trafficking plays an essential role in VEGF signaling and angiogenesis (34–36) and endoglin appears to regulate cellular levels of VEGFR2 in a VEGF-A–dependent manner (Fig. 2*A, D* and Supplemental Fig. 2*B, D*), we examined whether endoglin-regulated VEGF-A signaling and biology are through regulation of VEGFR2 trafficking. MEECs$^{-/-}$ transfected with EV or endoglin (**Fig. 5*A, B***) and MEECs$^{+/+}$ or MEECs$^{-/-}$ Supplemental Fig. 5*A, B*) were biotinylated at 4°C to prevent internalization. The biotinylated cells were treated with VEGF-A at 37°C to promote internalization and then were treated with trypsin to cleave uninternalized cell surface proteins. After IP with VEGFR2 antibody, the internalized VEGFR2 were detected using streptavidin-horseradish peroxidase. Although VEGF-A induced internalization of VEGFR2 in MEECs$^{-/-}$ (Fig. 5*A, B* and Supplemental Fig. 5*A, B*), VEGF-A induced less VEGFR2 internalization in MEECs$^{+/+}$ and MEECs$^{-/-}$ overexpressing endoglin (Fig. 5*A, B*). Further, overexpression of WT endoglin in MEECs$^{-/-}$ inhibited VEGFR2 internalization, whereas N3 and N6 mutant endoglin were less effective in inhibiting VEGFR2 internalization (Fig. 5*C, D*). As internalized VEGFR2 is usually degraded (36), we observed that treatment with VEGF-A for 3, 6, and 12 h induced a decrease in VEGFR2 levels in MEECs$^{-/-}$ but had a minimal effect on VEGFR2 levels in MEECs$^{+/+}$ (Fig. 5*E, F*). Consistently, treatment of HMEC-1s with VEGF-A for 12 h dramatically decreased VEGFR2 levels in HMEC-1-sh*ENG* cells but not in HMEC-1-shNTCs (Supplemental Fig. 5*C*). In addition, the basal VEGFR2 mRNA levels in HMEC-1-shNTC and MEECs$^{+/+}$ were higher than HMEC-1-sh*ENG* cells and MEECs$^{-/-}$ (Supplemental Fig. 5*D, E*). However, treatment with VEGF-A had no effect on VEGFR2 mRNA levels in HMEC-1-shNTCs and -sh*ENG* cells and MEECs$^{+/+}$, whereas increased VEGFR2 mRNA level in MEECs$^{-/-}$, suggesting that VEGF-A induced decreases in VEGFR2 levels in HMEC-1-sh*ENG* cells and MEECs$^{-/-}$ was not due to transcriptional regulation. Further, the lysosome inhibitor, leupeptin, but not the proteasome inhibitor, MG132, partially inhibited VEGF-A–induced VEGFR2 degradation in MEECs$^{-/-}$ and increased basal- and VEGF-A–induced VEGFR2 level in MEECs$^{+/+}$ (Supplemental Fig. 5*F*), suggesting that VEGF-A–induced internalized VEGFR2 is degraded in the lysosome. Finally, human WT endoglin rescued VEGF-A–induced VEGFR2 degradation, whereas endoglin N3 and N6 mutants that were deficient in interacting with VEGFR2 (Fig. 3*G, H*) did not (Fig. 5*G, H*). These data support a model in which endoglin promotes cell surface retention of VEGFR2 by inhibiting VEGF-A–mediated internalization and lysosomal degradation of VEGFR2.

Endoglin- and VEGF-targeting mAbs cooperate to inhibit sprouting *in vitro*

TRC105 is a chimeric IgG1 antibody that binds human endoglin and murine endoglin, albeit with lower affinity, and is in development as an antiangiogenic therapy (37–40). Because we have determined that

prepared. *F*) HA-endoglin and VEGFR2 were detected in IP and total cell lysates by Western blot analysis. Results are representative of 3 independent experiments. *G, H*) MEEC$^{-/-}$ cells were transfected with VEGFR2 and indicated HA-endoglin NAAIRS mutants for 24 h. Anti-HA IPs were prepared. HA-endoglin and VEGFR2 were detected in IP and total cell lysates by Western blot analysis. The ratio of VEGFR2 to endoglin in the IPs is represented as VEGFR2/endoglin interaction and expressed relative to the VEGFR2/endoglin value in WT endoglin-expressing cells (100%). Data are means ± SEM of results in 4 experiments. ****$P < 0.0001$ (2-tailed Student's *t* test).

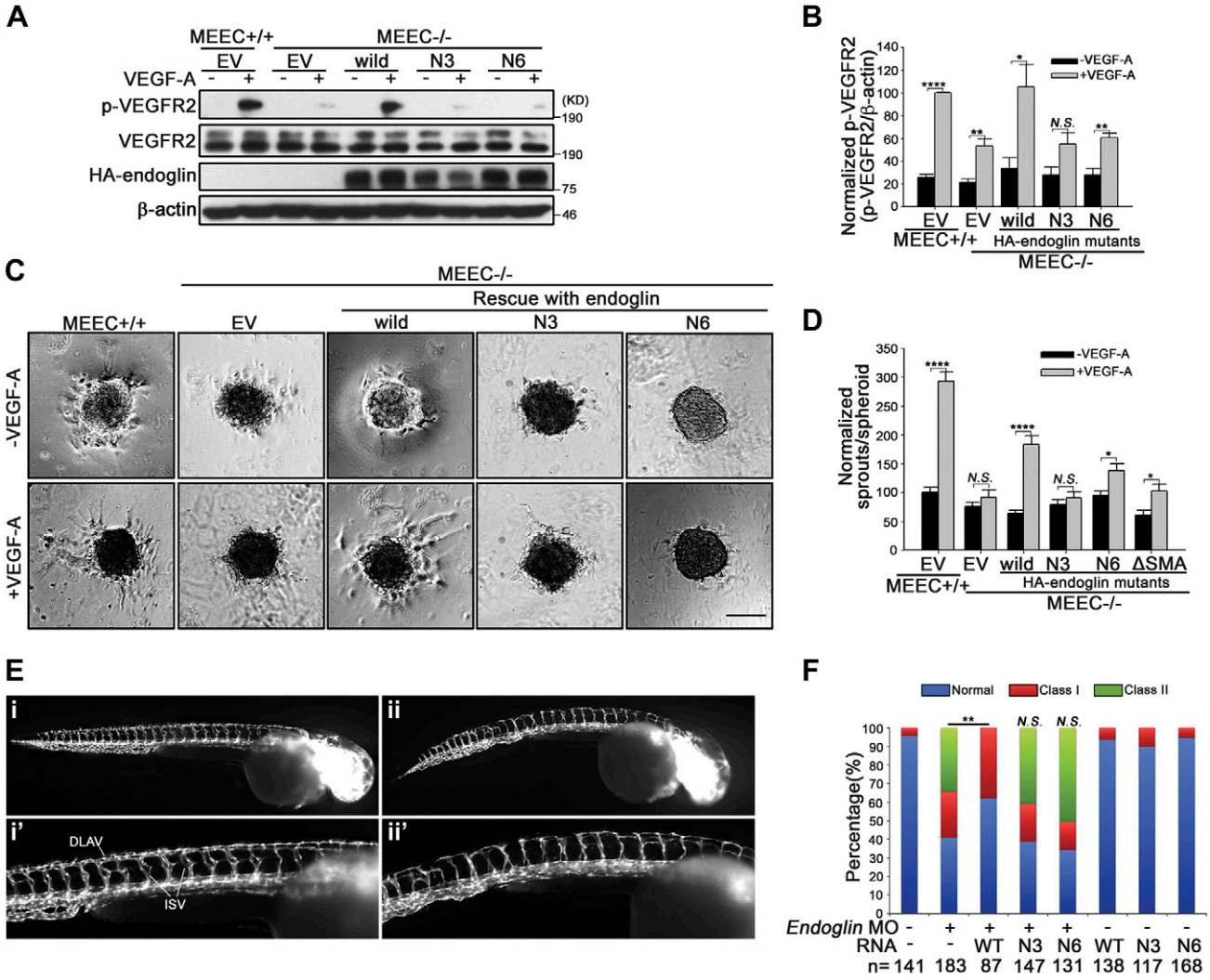

Figure 4. Endoglin and VEGFR2 interaction promotes VEGF-A–induced angiogenesis and VEGF signaling. *A*, *B*) MEECs$^{+/+}$ and MEECs$^{-/-}$ transfected with EV, WT endoglin, or mutant endoglin N3 or N6 were serum starved for 6 h and treated with 50 ng/ml VEGF-A for 5 min, and the cell lysates were analyzed with the indicated antibodies. p-VEGFR2/β-actin levels in MEECs$^{+/+}$ treated with VEGF-A were normalized to 100, and the p-VEGFR2/β-actin levels of other conditions were calculated relative to this value. Data are means ± SEM of 3 experiments. $*P < 0.05$, $**P < 0.01$, $****P < 0.0001$ (2-tailed Student's *t* test). *C*, *D*) Endothelial spheroids made from MEECs$^{+/+}$ and MEECs$^{-/-}$ transfected with EV, WT endoglin, mutant endoglin N3 or N6 were treated with or without 100 ng/ml VEGF-A and cultured on Matrigel for 18 h. The mean value of the number of sprouts in the MEECs$^{+/+}$ without treatment was normalized to 100, and the sprouting of other conditions was calculated relative to this value. Data are means ± SEM of results in 3 experiments. $*P < 0.05$, $****P < 0.0001$ (2-tailed Student's *t* test). Scale bar, 300 μm. *E*, *F*) Representative photographs of Fli1-EGFP control embryos (*Ei*) and embryos injected with endoglin MO (*Eii*) at 48 hpf, as visualized by fluorescence microscopy. *Ei'*, *ii'*) Higher magnifications of the trunk. *F*) Percentage of normal embryos and embryos with ISV sprouting defects defined as class I (1–3 ISVs affected and class II (3+ ISVs affected). A χ^2 test was performed as follows: MO *vs.* MO+RNA WT ($P = 0.0015$); MO *vs.* MO+RNA N3 ($P = 0.7634$); MO *vs.* MO+N6 ($P = 0.1182$). Data are means ± SEM of 3 experiments. N.S., not significant. $**P < 0.01$.

endoglin promotes VEGF signaling and VEGF-induced sprouting and angiogenesis, we asked whether TRC105 cooperates with anti-VEGF therapy to inhibit angiogenesis. TRC105 dose dependently inhibited VEGF-A–induced VEGFR2 phosphorylation (Tyr 1175) in both MEECs$^{+/+}$ (**Fig. 6*A***) and HMEC-1s (Fig. 6*B*). Further, the combination of TRC105 and a human VEGF-A mAb, bevacizumab, further inhibited VEGF-A–induced VEGFR2 phosphorylation compared with pretreatment of either agent alone in MEECs$^{+/+}$ (Tyr 1175; Fig. 6*C*, *D*). In addition, in the presence of TRC105, treatment with VEGF-A for 12 h decreased VEGFR2 level in WT MEECs (Fig. 6*E*, *F*), phenocopying the effects of loss of endoglin (Fig. 5*E*, *F* and Supplemental Fig. 5*C*). As Matrigel is extracted from the Engelbreth-Holm-Swarm mouse sarcoma, a tumor rich in extracellular matrix proteins including laminin, collagen IV, heparin sulfate proteoglycans, entactin/nidogen, and several growth factors, it can effectively mimic the tumor microenvironment. Accordingly, we assessed the effect of TRC105 and a mouse VEGF-A mAb, B20-4.1 on endothelial sprouting in Matrigel. Although both TRC105 and B20-4.1 decreased

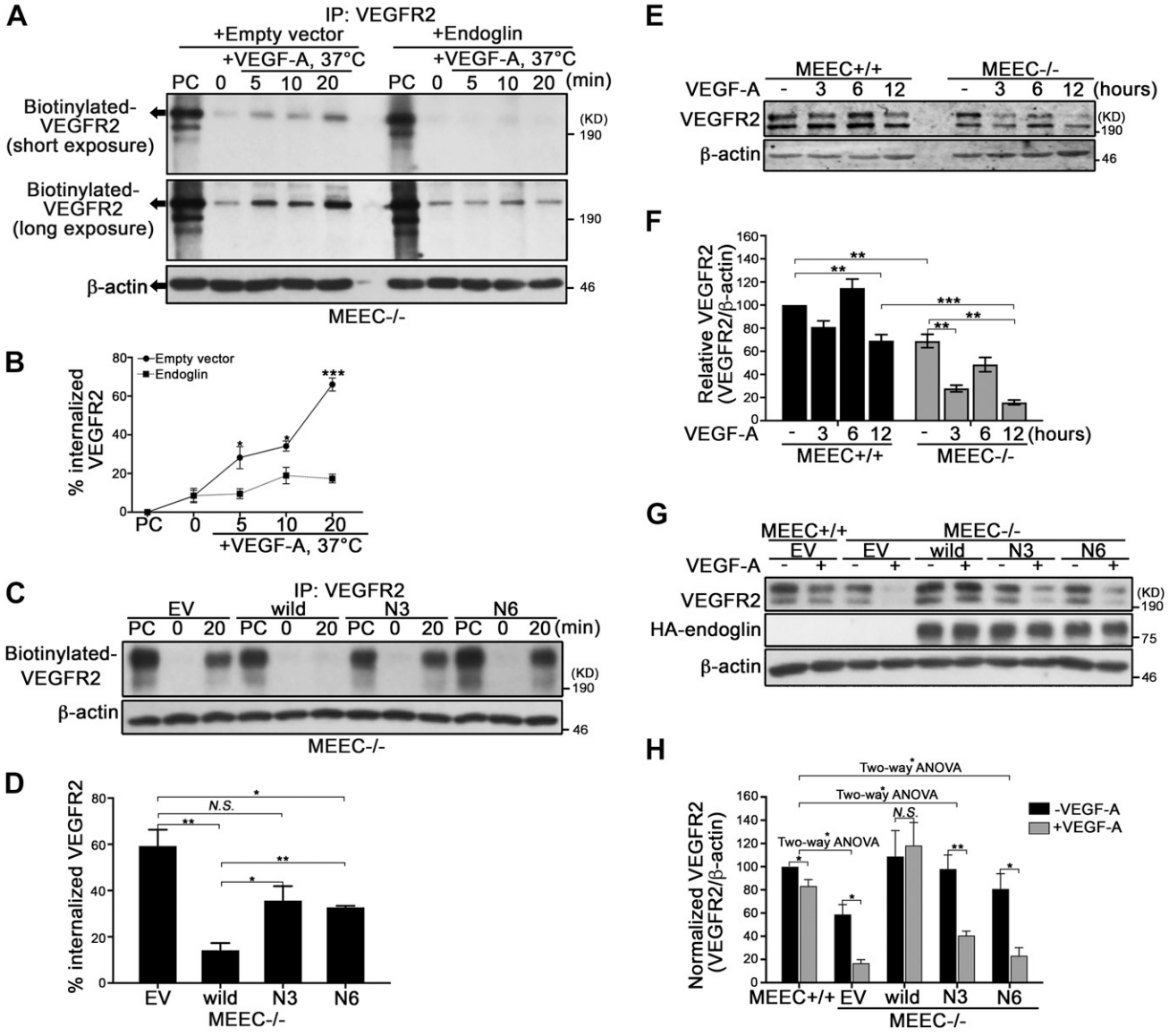

Figure 5. Endoglin prevented VEGF-A–induced VEGFR2 internalization and degradation. *A*, *B*) MEECs$^{-/-}$ were transfected with empty vector or HA-endoglin together with VEGFR2 for 24 h, and cell surface proteins were labeled with sulfo-NHS-LC-biotin for 2 h at 4°C. Cells were then treated with 50 ng/ml VEGF-A at 37°C for the indicated time, to promote the internalization of cell surface proteins, and then treated with trypsin to cleave the uninternalized cell surface proteins. The cells were lysed and immunoprecipitated with anti-VEGFR2 antibody, proteins were resolved by SDS-PAGE, and the internalized biotinylated VEGFR2 was blotted with streptavidin-horseradish peroxidase. The surface VEGFR2 without trypsin digestion was used as a positive control (PC), with values set at 0%; the surface VEGFR2 without VEGF, which was directly treated with trypsin (0), was used as a negative control. Means ± SEM of results in 3 experiments. $^{*}P < 0.05$, $^{***}P < 0.001$ (2-tailed Student *t* test). *C*, *D*) MEECs$^{+/+}$ or MEECs$^{-/-}$ transfected with EV, WT endoglin, mutant endoglin N3 or N6, together with VEGFR2 for 24 h, and cell surface proteins were labeled with sulfo-NHS-LC-biotin for 2 h at 4°C. VEGFR2 internalization assays were performed as previously described. Data are means ± SEM of results in 3 experiments. NS, not significant. $^{*}P < 0.05$, $^{**}P < 0.01$ (Student's *t* test). *E*, *F*) MEECs$^{+/+}$ and MEECs$^{-/-}$ were treated with 100 ng/ml VEGF-A for the indicated times, and the cell lysates were analyzed with the indicated antibodies. VEGFR2/β-actin level in MEECs$^{+/+}$ without treatment was normalized to 100, and the VEGFR2/β-actin levels of other conditions were calculated relative to this value. Data are means ± SEM of results in 3 experiments. $^{**}P < 0.01$, $^{***}P < 0.001$ (2-tailed Student *t* test). *G*, *H*) MEECs$^{+/+}$ or MEECs$^{-/-}$ transfected with EV, WT endoglin, and mutant endoglin N3 or N6 were treated with 100 ng/ml VEGF-A for 12 h, and the cell lysates were analyzed with the indicated antibodies. VEGFR2/β-actin level in MEECs$^{+/+}$ without treatment was normalized to 100, and the VEGFR2/β-actin levels of other conditions were calculated relative to this value. Data are means ± SEM of results in 3 experiments. NS, not significant. $^{*}P < 0.05$ (2-tailed Student's *t* test, and the statistical interaction between VEGF-A treatment; and different endoglin mutants' expression was obtained by 2-way ANOVA).

sprouting, the combination of TRC105 and B20-4.1 further inhibited sprouting (Fig. 6*G*, *H*). Thus, endoglin and VEGF-A targeting mAbs cooperate to inhibit VEGF signaling and VEGF-induced sprouting *in vitro*.

TRC105 enhances anti-VEGF therapy *in vivo*

To assess whether TRC105 enhances anti-VEGF therapy *in vivo*, we injected 4T1 cells into the inguinal mammary fat

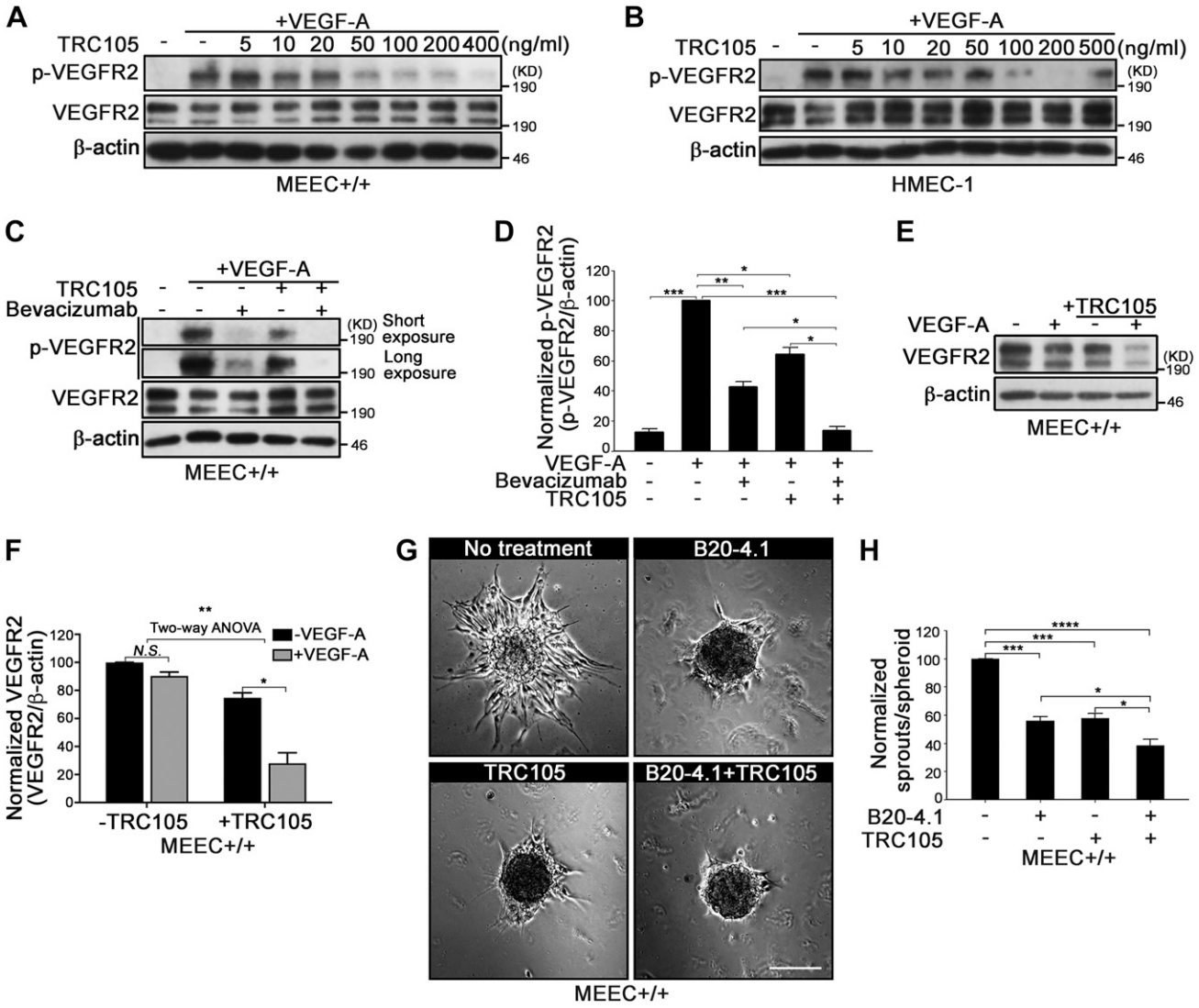

Figure 6. TRC105 cooperates with bevacizumab to inhibit VEGF pathway. MEECs$^{+/+}$ (*A*) or HMEC-1s (*B*) were serum starved for 6 h, pretreated with the indicated doses of TRC105 for 1 h, and then treated with 50 ng/ml VEGF-A for 5 min. The cell lysates were analyzed with the indicated antibodies. Results are representative of 3 independent experiments. *C*, *D*) MEECs$^{+/+}$ were serum starved for 6 h, pretreated with 5 ng/ml bevacizumab, with or without 200 ng/ml TRC105 for 1 h, and then treated with 50 ng/ml VEGF-A for 5 min; the cell lysates were analyzed with the indicated antibodies. The p-VEGFR2/β-actin level in MEEC$^{+/+}$ cells treated with VEGF-A was normalized to 100, and the p-VEGFR2/β-actin levels of other conditions were calculated relative to this value. Means ± SEM of results in 3 experiments. *$P < 0.05$, **$P < 0.01$, ***$P < 0.001$ (2-tailed Student's *t* test). *E*, *F*) MEECs$^{+/+}$ were treated with 100 ng/ml VEGF-A, with or without 200 ng/ml TRC105 for 12 h, and the cell lysates were analyzed with the indicated antibodies. The VEGFR2/β-actin level in MEECs$^{+/+}$ without treatment was normalized to 100, and the VEGFR2/β-actin levels of other conditions were calculated relative to this value. Quantitative data are means ± SEM of results 3 independent experiments. NS, not significant. *$P < 0.05$, **$P < 0.01$ (2-tailed Student's *t* test, and the statistical interaction between VEGF-A and TRC105 treatment was obtained by 2-way ANOVA). *G*, *H*) MEEC$^{+/+}$ endothelial spheroids were cultured on Matrigel, treated with or without 5 ng/ml B20-4.1, with or without 200 ng/ml TRC105 for 18 h. The number of sprouts in the MEECs$^{+/+}$ without treatment was normalized to 100, and the sprouting of other condition was calculated relative to this value. The number of sprouts (*H*) was quantified using image analysis. Data are means ± SEM of results in 3 experiments. *$P < 0.05$, ***$P < 0.001$, ****$P < 0.0001$. Scale bar, 300 μm.

pads of nude mice and began treatment with TRC105, with or without B20-4.1, 1 wk after injection (**Fig. 7*A***). Treatment with either TRC105 or B20-4.1 inhibited tumor growth, and combination treatment with TRC105 and B20-4.1 further decreased growth (Fig. 7*B*). In addition, the combination treatment decreased tumor size (Fig. 7*C*) and tumor weight (Fig. 7*D*) compared with the tumors in untreated mice or in mice treated with either agent alone. Further, the combination treatment inhibited metastasis to the lung as monitored by IVIS scanning (Supplemental Fig. 6 and **Table 1**). Consistently, the combination treatment of B20-4.1 and TRC105 decreased the size of metastatic lung tumors compared to no treatment or treatment with either agent alone (Fig. 7*E*, *F*). Finally, staining for the endothelial marker CD31 demonstrated that combination treatment with B20-4.1 and TRC105 further decreased tumor-associated angiogenesis compared with treatment with either

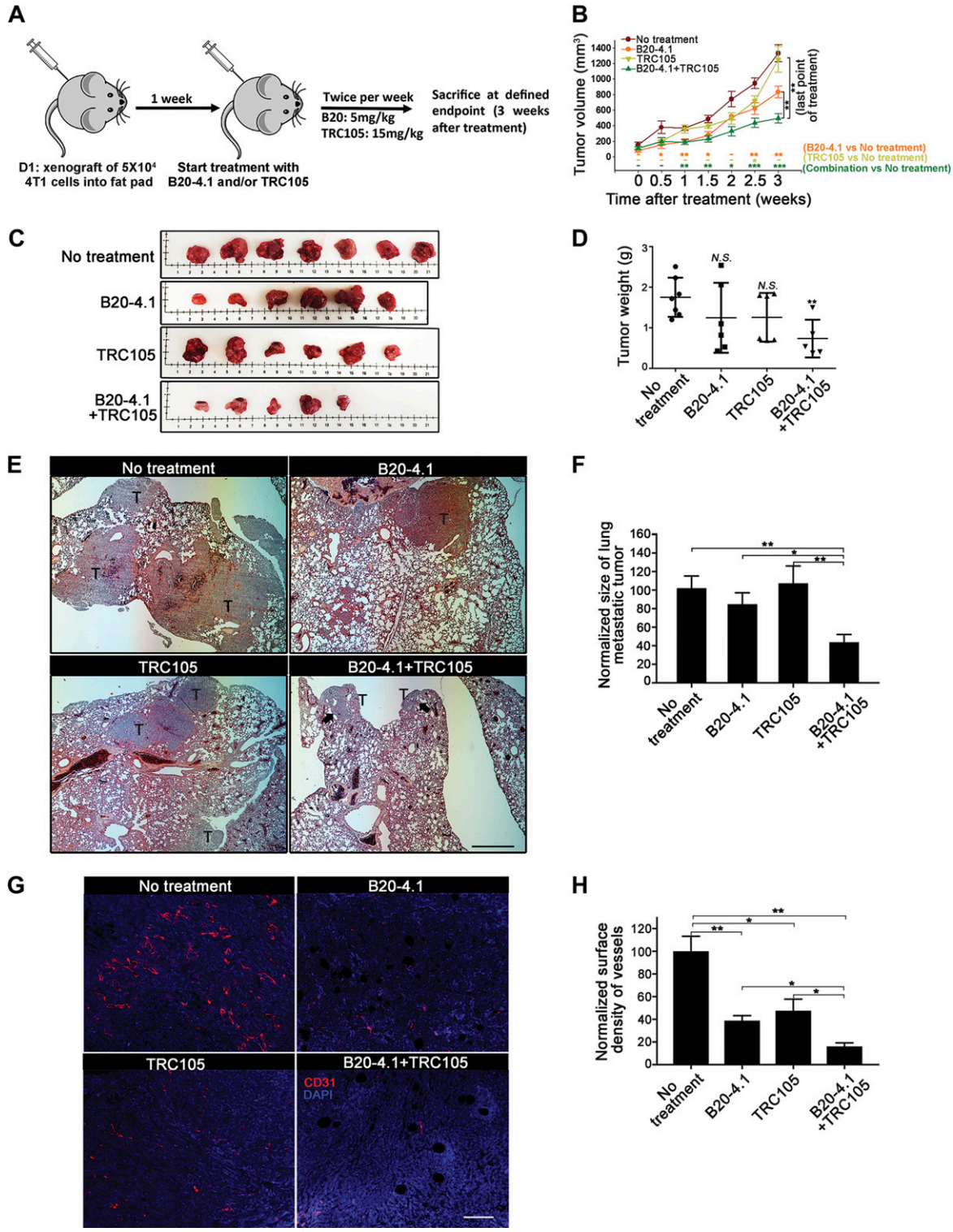

Figure 7. TRC105 enhances anti-VEGF therapy *in vivo*. *A*) The murine model. *B–D*) 4T1 cells were implanted into the inguinal mammary fat pads of female nude mice, treated with B20-4.1, with or without TRC105 twice per week. Primary tumor growth was recorded by measuring tumor size twice per week after injection. Data are means ± SEM (*B*), and tumor weight was measured as means ± SEM after mice were euthanized (*C*, *D*). N.S., not significant. $*P < 0.05$, $**P < 0.01$, $***P < 0.001$ (2-tailed Student's *t* test). *E*, *F*) Hematoxylin and eosin staining for the lung tissue sections. The size of the metastatic tumor in lung of untreated mice was normalized to 100, and the size of metastatic tumors in the lung of other conditions were calculated relative to those in the untreated mice. Data are means ± SEM. $*P < 0.05$, $**P < 0.01$ (2-tailed Student's *t* test). Scale bar, 1.5 mm. *G*, *H*) CD31 staining for the primary tumor sections, the nuclei were stained with DAPI. The surface density of vessels (measured as the total area of blood vessels occupied in each field) in the primary tumor of the untreated mice was normalized to 100, whereas the surface density of vessels in the other conditions were calculated relative to the untreated mice. Data are means ± SEM. $P < 0.05$, $**P < 0.01$ (2-tailed Student's *t* test). Scale bar, 100 μm.

TABLE 1. *Local invasion and distant metastasis of the murine model*

Treatment	Local invasion	Distant metastasis
No treatment	3/7	4/7
B20-4.1	2/6	3/6
TRC105	3/6	1/6
B20-4.1+TRC105	1/5	1/5

agent alone (Fig. 7*G*, *H*). These data indicate that TRC105 enhances B20-4.1's effects to inhibit tumor growth, metastasis, and tumor-associated angiogenesis, and suggests that TRC105 enhances the anti-angiogenic effects of anti-VEGF therapy *in vivo*.

DISCUSSION

In this study, endoglin, a TGF-β superfamily coreceptor, regulated VEGF signaling and biology in endothelial cells and in vascular development *in vitro* and *in vivo*. Mechanistically, endoglin and VEGFR2 formed a complex at the cell surface thereby preventing VEGFR2 internalization and degradation, increasing VEGFR2 cell surface stability, which may contribute to maintaining the tip cell phenotype (**Fig. 8**).

Endoglin's effects on endothelial cell biology have traditionally been thought to be through ALK1, as endoglin enhances ALK1/Smad1/5/8 signaling (24, 41). However, several lines of evidence suggest that endoglin has ALK1-independent effects. For example, endoglin and ALK1 heterozygous mice have distinct pulmonary and hepatic angiogenic profiles and different responses to anti-VEGF-A treatment (42). In this study, we demonstrated that endoglin independently enhances VEGF-A signaling and biology, including sprouting. In addition, single-site mutants for 3 endoglin phosphorylation sites by ALK5 (S643, S646, and S647) (33) or the NAAIRS mutant (N5) which contains 2 phosphorylation sites by ALK1 (S634 and S635) (43) did not decrease the VEGFR2/endoglin interaction. However, in contrast to endoglin promoting VEGF induced sprouting, BMP-9/ALK1 signaling has been demonstrated to suppress sprouting by cooperating with Notch signaling, without regulating the VEGF pathway (44, 45). Hence, ALK1 and endoglin may coordinately but independently regulate the VEGF-A/Notch signaling balance to determine endothelial cell fate, either as tip or stalk cells.

The BMP-9/ALK1/Smad1/5/8 pathway is generally regarded as a vascular quiescence factor with a role in the resolution phase of angiogenesis (11). Endoglin, as a coreceptor for ALK1, also stabilizes newly formed blood vessels. In our study, the BMP-9/ALK1/endoglin pathway enhanced endothelial capillary tube stability by promoting the PI3K/Akt pathway (46) and crosstalk with the fibronectin/integrin α5β1 pathway (24), to protect endothelial cells from apoptosis. However, the present work is in the context of endothelial sprouting, an early stage of the activation phase of angiogenesis, in which VEGF signaling plays a predominant role. Here, endoglin's roles may be mediated largely through effects on the VEGF pathway, independent of the BMP-9/ALK1 pathway. In terms of TRC105's effect in breast cancer progression demonstrated in this study, when TRC105 binds the extracellular domain of endoglin, it may make endoglin inaccessible to VEGFR2, disrupting the endoglin/VEGFR2 interaction and promoting subsequent VEGFR2 internalization and degradation. Because TRC105 is an endoglin antibody, we cannot assess its effect on endoglin/VEGFR2 interaction directly using coimmunoprecipitation or PLAs because TRC105 would compete with the endoglin antibody used in these 2 assays. However, we demonstrated that TRC105 inhibits VEGF-A–induced VEGFR2 phosphorylation in the short-term (5 min) while promoting VEGFR2 degradation with long-term (12 h) VEGF-A stimulation. These data suggest that endoglin promotes different stages of angiogenesis *via* different mechanisms, promoting endothelial sprouting at early stages through effects on VEGF pathway while stabilizing newly formed blood vessels through effects on PI3K/Akt and fibronectin/integrin α5β1 pathways.

In terms of how endoglin regulates VEGF signaling and biology, we established that endoglin interacts with VEGFR2 through its cytoplasmic domain. The interaction with endoglin sustains VEGFR2 on the cell surface and enhances the extent of VEGFR2 activation. This is consistent with a recent report demonstrating that knockdown of endoglin promotes VEGFR2 clearance from the plasma membrane (20). In addition, investigation of VEGFR2/endoglin interaction *in vivo* is very informative. However, assessing coimmunoprecipitation of endogenous endoglin/VEGFR2 is difficult as endoglin

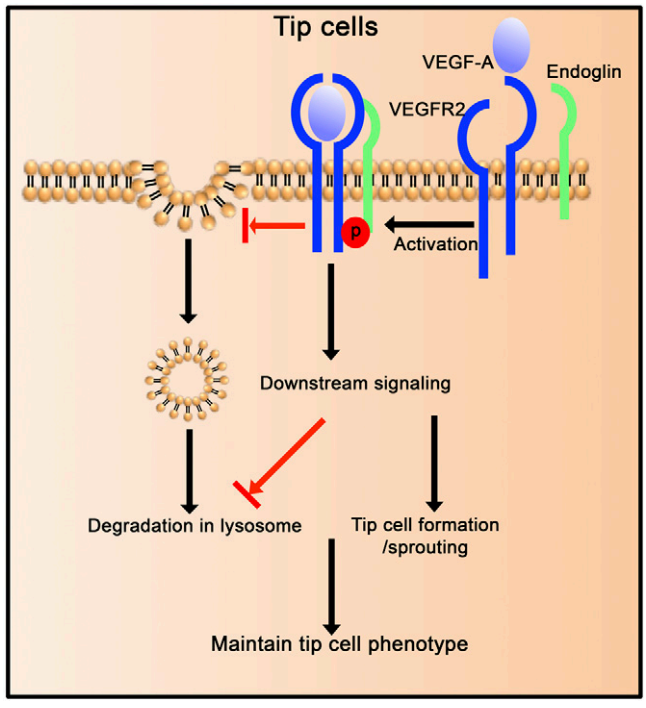

Figure 8. Model of endoglin-regulated VEGF-A–induced sprouting. In tip cells, endoglin sustains VEGFR2 on the cell surface, preventing its degradation in lysosomes. This results in tip cells remaining responsive to VEGF as they probe the VEGF gradient facilitating blood vessel elongation during angiogenesis.

expression is very low in endothelial cells. As an alternative approach, we performed the PLAs, which allow us to detect the interaction of endogenous receptors *in situ.* VEGFR2 internalization is necessary for VEGF signal transduction (35, 47). Although loss of endoglin promotes VEGFR2 internalization, it also promotes VEGFR2 trafficking to the lysosome and degradation (Fig. 8). These findings suggest that endoglin regulates VEGFR2 internalization and fate determination between activation and degradation. We observed that loss of endoglin decreased basal the VEGFR2 level in MEECs$^{-/-}$ compared with MEECs$^{+/+}$ (Fig. 2*A*, *D*, *F*, *H*, *J* and Supplemental Fig. 2*H*, *N*), but not in HMEC-1-sh*ENG* cells compared with HMEC-1-shNTCs (Supplemental Fig. 2*B*, *D*, *J*). Consistent with this observation, the VEGFR2 mRNA level in MEECs$^{-/-}$ is much lower than in MEECs$^{+/+}$ (Supplemental Fig. 5*E*), whereas the VEGFR2 mRNA in HMEC-1-sh*ENG* cells was only slightly lower than that in shNTCs (Supplemental Fig. 5D). This difference may also be related to the MEEC, but not the HMEC-1 medium, containing VEGF-A, which could mediate internalization and degradation of VEGFR2 in the absence of endoglin expression, as demonstrated in this study.

Endothelial cells involved in angiogenesis are heterogeneous. Tip cells express high levels of VEGFR2 to probe the VEGF gradient in the angiogenic microenvironment leading to elongation of blood vessels. This probing requires VEGFR2 to be stably expressed on the tip cells during sprouting and vessel elongation. Studies have shown that endoglin is strongly expressed in the stalk cells, and weakly in the tip cells (20, 48). However, we and another laboratory demonstrated that loss of endoglin reduces tip cell potential (20), while overexpressing endoglin leads to a strong overrepresentation in the tip cell position (20). These suggest that endoglin is important to promote and maintain the tip cell phenotype. As we demonstrated, endoglin prevents VEGF-A–induced VEGFR2 internalization and degradation in endothelial cells (Fig. 5*E*, *F* and Supplemental Fig. 5C), which is a potential mechanism by which endoglin functions to maintain the tip cell phenotype (Fig. 8).

There are several studies on the role of endoglin, TGF-β signaling, and VEGF signaling in the literature that highlight the importance and complexity of these pathways in angiogenesis. However, some of these studies have supported different and sometime opposing conclusions on the role of these pathways, perhaps because of differences in the cellular context of the studies. For example, Jin *et al.* (20) showed that loss of endoglin is associated with hyperactivation of the VEGFR2 downstream component AKT, but not ERK. In contrast, we demonstrated that loss of endoglin decreases ERK activation, perhaps because of differences in the endothelial cell lines (HMEC-1s and MEECs$^{+/+}$ *vs.* human dermal (HD)MECs). Second, the differences may be related to the use of different technical approaches. For example, we have demonstrated that loss of endoglin by suppressing endogenous endoglin translation *via* endoglin-MOs in *Fli1-EGFP* embryos caused significant defects in the formation of both ISVs and the DLAV, whereas another laboratory demonstrated that endoglin mutation with a frameshift after 15 aa and premature stop codons after 61 aa show no major defects in sprouting (21). Finally, the cell heterogeneous angiogenic microenvironment may explain the different results from *in vitro* and *in vivo* studies. Most *in vitro* research studies have used monolayer endothelial cells to investigate the cell signaling during angiogenesis, which cannot capture endothelial functions during in angiogenesis *in vivo*, including tip, stalk, and phalanx cell specification. In addition, the angiogenic microenvironment is very complicated, consisting of many angiogenic factors, anti-angiogenic factors, and a host of other types of cells including pericytes, vascular smooth muscle cells, and immune components. The angiogenic effect is the integrated effects of all these factors. However, most *in vitro* studies investigate one or several of these factors, which can result in differences from *in vivo* studies. Although *in vivo* studies are highly informative and should be prioritized, the clean background of *in vitro* studies provides valuable information, especially in the study of specific signaling pathways.

Because both endoglin and VEGF-A are involved in human diseases, including HHT and cancer, the interaction between endoglin and the VEGF pathway established in this study provides a rationale for development of novel treatment strategies for these diseases. For example, the VEGF-A mAb bevacizumab is under clinical investigation to treat HHT (49). Treating HHT with bevacizumab reduces the frequency and intensity of epistaxis, gastrointestinal bleeding episodes, and liver arteriovenous malformations. Moreover, VEGF inhibitors, including bevacizumab, sunitinib, and sorafenib, have been used to treat cancer by targeting tumor-associated angiogenesis. However, these drugs have modest effects on overall survival because of therapy resistance (50–52). One report indicated that TRC105 failed to improve progression-free survival in patients with treated renal cell cancers who were receiving bevacizumab (53), but a recent publication demonstrated that tumors deprived of endoglin exhibited a delayed onset of resistance to anti-VEGF-A agents (54) and another demonstrated that targeting endoglin and the VEGF pathway with TRC105 and the VEGF receptor kinase inhibitor SU-5416 inhibited tumor angiogenesis and metastatic spread in breast cancer models (55). However, besides VEGFR2, SU-5416 also targets Fms-related tyrosine kinase-3 (56) and c-kit (57). In our study, we used B20-4.1, a murine VEGF-A–specific mAb. These studies and ours support the promise of combining anti-VEGF-A and anti-endoglin agents to treat cancer. The findings in the current study, which identify the detailed mechanism by which endoglin regulates VEGF signaling and biology, underscore this promise. Further, endoglin is an endothelial coreceptor of TGF-β pathway, which is another important angiogenic pathway. Thus, anti-endoglin and anti-VEGF agents may work together to inhibit VEGF signaling and, in parallel, to inhibit endoglin and VEGFR independent signaling functions. Indeed, an open-label phase Ib study (NCT01332721) has demonstrated that TRC105 can be safely combined with bevacizumab at the recommended single-agent doses of each drug. The combination also demonstrated durable activity in a VEGF inhibitor–refractory population (58). Regardless of the outcome of these early studies, the mechanistic insights into VEGF

and endoglin signaling and crosstalk demonstrated in out study will provide avenues to explore initial or required resistance or to inform subsequent trials.

In summary, this study identified a novel mechanism by which endoglin regulates VEGF signaling and biology, forming a rational framework for deciphering responses to agents that target these pathways in human disease. FJ

ACKNOWLEDGMENTS

The authors thank Dr. Elisabetta Dejana [Italian Foundation for Cancer Research (FIRC) Institute of Molecular Oncology, European Institute of Oncology, Milan, Italy] for providing mouse embryonic endothelial cells; Dr. Christopher D. Kontos (Duke University) for providing the VEGFR2 construct; Tracon Pharma, Inc. (San Diego, CA, USA) for providing TRC105 antibody; and Genentech, Inc. for providing bevacizumab and B20-4.1 antibodies. This work was supported, in part, by Susan G. Komen for the Cure Grants CCR15333124 (to H.T.) and SAC10002 (to G.C.B.), and an HHT Young Scholar Award (to H.T.). The authors declare no conflicts of interest.

AUTHOR CONTRIBUTIONS

H. Tian, C. Golzio, N. Katsanis, and G. C. Blobe designed the experiments; H. Tian, J. J. Huang, C. Golzio, and X. Gao conducted the experiments and analyzed the data; M. Hector-Greene provided resources and materials; H. Tian and G. C. Blobe wrote the manuscript; and all authors discussed the results and edited the final manuscript.

REFERENCES

1. Nagy, J. A., Dvorak, A. M., and Dvorak, H. F. (2007) VEGF-A and the induction of pathological angiogenesis. *Annu. Rev. Pathol.* **2**, 251–275
2. Gerhardt, H., Golding, M., Fruttiger, M., Ruhrberg, C., Lundkvist, A., Abramsson, A., Jeltsch, M., Mitchell, C., Alitalo, K., Shima, D., and Betsholtz, C. (2003) VEGF guides angiogenic sprouting utilizing endothelial tip cell filopodia. *J. Cell Biol.* **161**, 1163–1177
3. Hellström, M., Phng, L. K., Hofmann, J. J., Wallgard, E., Coultas, L., Lindblom, P., Alva, J., Nilsson, A. K., Karlsson, L., Gaiano, N., Yoon, K., Rossant, J., Iruela-Arispe, M. L., Kalén, M., Gerhardt, H., and Betsholtz, C. (2007) Dll4 signalling through Notch1 regulates formation of tip cells during angiogenesis. *Nature* **445**, 776–780
4. Lobov, I. B., Renard, R. A., Papadopoulos, N., Gale, N. W., Thurston, G., Yancopoulos, G. D., and Wiegand, S. J. (2007) Delta-like ligand 4 (Dll4) is induced by VEGF as a negative regulator of angiogenic sprouting. *Proc. Natl. Acad. Sci. USA* **104**, 3219–3224
5. Pardali, E., and ten Dijke, P. (2009) Transforming growth factor-beta signaling and tumor angiogenesis. *Front. Biosci.* **14**, 4848–4861
6. Goumans, M. J., Liu, Z., and ten Dijke, P. (2009) TGF-beta signaling in vascular biology and dysfunction. *Cell Res.* **19**, 116–127
7. Massagué, J. (1998) TGF-beta signal transduction. *Annu. Rev. Biochem.* **67**, 753–791
8. Goumans, M. J., Valdimarsdottir, G., Itoh, S., Rosendahl, A., Sideras, P., and ten Dijke, P. (2002) Balancing the activation state of the endothelium via two distinct TGF-beta type I receptors. *EMBO J.* **21**, 1743–1753
9. Goumans, M. J., Lebrin, F., and Valdimarsdottir, G. (2003) Controlling the angiogenic switch: a balance between two distinct TGF-b receptor signaling pathways. *Trends Cardiovasc. Med.* **13**, 301–307
10. David, L., Mallet, C., Mazerbourg, S., Feige, J. J., and Bailly, S. (2007) Identification of BMP9 and BMP10 as functional activators of the orphan activin receptor-like kinase 1 (ALK1) in endothelial cells. *Blood* **109**, 1953–1961
11. David, L., Mallet, C., Keramidas, M., Lamandé, N., Gasc, J. M., Dupuis-Girod, S., Plauchu, H., Feige, J. J., and Bailly, S. (2008) Bone morphogenetic protein-9 is a circulating vascular quiescence factor. *Circ. Res.* **102**, 914–922
12. Li, D. Y., Sorensen, L. K., Brooke, B. S., Urness, L. D., Davis, E. C., Taylor, D. G., Boak, B. B., and Wendel, D. P. (1999) Defective angiogenesis in mice lacking endoglin. *Science* **284**, 1534–1537
13. Oh, S. P., Seki, T., Goss, K. A., Imamura, T., Yi, Y., Donahoe, P. K., Li, L., Miyazono, K., ten Dijke, P., Kim, S., and Li, E. (2000) Activin receptor-like kinase 1 modulates transforming growth factor-beta 1 signaling in the regulation of angiogenesis. *Proc. Natl. Acad. Sci. USA* **97**, 2626–2631
14. McAllister, K. A., Grogg, K. M., Johnson, D. W., Gallione, C. J., Baldwin, M. A., Jackson, C. E., Helmbold, E. A., Markel, D. S., McKinnon, W. C., Murrell, J., Mccormick, M. K., Pericakvance, M. A., Heutink, P., Oostra, B. A., Haitjema, T., Westerman, C. J. J., Porteous, M. E., Guttmacher, A. E., Letarte, M., and Marchuk, D. A. (1994) Endoglin, a TGF-beta binding protein of endothelial cells, is the gene for hereditary haemorrhagic telangiectasia type 1. *Nat. Genet.* **8**, 345–351
15. McDonald, J., Bayrak-Toydemir, P., and Pyeritz, R. E. (2011) Hereditary hemorrhagic telangiectasia: an overview of diagnosis, management, and pathogenesis. *Genet. Med.* **13**, 607–616
16. Minhajat, R., Mori, D., Yamasaki, F., Sugita, Y., Satoh, T., and Tokunaga, O. (2006) Endoglin (CD105) expression in angiogenesis of colon cancer: analysis using tissue microarrays and comparison with other endothelial markers. *Virchows Arch.* **448**, 127–134
17. Hendriksen, E. M., Span, P. N., Schuuring, J., Peters, J. P. W., Sweep, F. C. G. J., van der Kogel, A. J., and Bussink, J. (2009) Angiogenesis, hypoxia and VEGF expression during tumour growth in a human xenograft tumour model. *Microvasc. Res.* **77**, 96–103
18. Li, C., Issa, R., Kumar, P., Hampson, I. N., Lopez-Novoa, J. M., Bernabeu, C., and Kumar, S. (2003) CD105 prevents apoptosis in hypoxic endothelial cells. *J. Cell Sci.* **116**, 2677–2685
19. Zhu, Y., Sun, Y., Xie, L., Jin, K., Sheibani, N., and Greenberg, D. A. (2003) Hypoxic induction of endoglin via mitogen-activated protein kinases in mouse brain microvascular endothelial cells. *Stroke* **34**, 2483–2488
20. Jin, Y., Muhl, L., Burmakin, M., Wang, Y., Duchez, A. C., Betsholtz, C., Arthur, H. M., and Jakobsson, L. (2017) Endoglin prevents vascular malformation by regulating flow-induced cell migration and specification through VEGFR2 signalling. *Nat. Cell Biol.* **19**, 639–652
21. Sugden, W. W., Meissner, R., Aegerter-Wilmsen, T., Tsaryk, R., Leonard, E. V., Bussmann, J., Hamm, M. J., Herzog, W., Jin, Y., Jakobsson, L., Denz, C., and Siekmann, A. F. (2017) Endoglin controls blood vessel diameter through endothelial cell shape changes in response to haemodynamic cues. *Nat. Cell Biol.* **19**, 653–665
22. Liu, Z., Lebrin, F., Maring, J. A., van den Driesche, S., van der Brink, S., van Dinther, M., Thorikay, M., Martin, S., Kobayashi, K., Hawinkels, L. J., van Meeteren, L. A., Pardali, E., Korving, J., Letarte, M., Arthur, H. M., Theuer, C., Goumans, M. J., Mummery, C., and ten Dijke, P. (2014) ENDOGLIN is dispensable for vasculogenesis, but required for vascular endothelial growth factor-induced angiogenesis. *PLoS One* **9**, e86273
23. Pece-Barbara, N., Vera, S., Kathirkamathamby, K., Liebner, S., Di Guglielmo, G. M., Dejana, E., Wrana, J. L., and Letarte, M. (2005) Endoglin null endothelial cells proliferate faster and are more responsive to transforming growth factor beta1 with higher affinity receptors and an activated Alk1 pathway. *J. Biol. Chem.* **280**, 27800–27808
24. Tian, H., Mythreye, K., Golzio, C., Katsanis, N., and Blobe, G. C. (2012) Endoglin mediates fibronectin/α5β1 integrin and TGF-β pathway crosstalk in endothelial cells. *EMBO J.* **31**, 3885–3900
25. Tian, H., Liu, J., Chen, J., Gatza, M. L., and Blobe, G. C. (2015) Fibulin-3 is a novel TGF-β pathway inhibitor in the breast cancer microenvironment. *Oncogene* **34**, 5635–5647
26. Tian, H., Ketova, T., Hardy, D., Xu, X., Gao, X., Zijlstra, A., and Blobe, G. C. (2017) Endoglin mediates vascular maturation by promoting vascular smooth muscle cell migration and spreading. *Arterioscler. Thromb. Vasc. Biol.* **37**, 1115–1126
27. Alajati, A., Laib, A. M., Weber, H., Boos, A. M., Bartol, A., Ikenberg, K., Korff, T., Zentgraf, H., Obodozie, C., Graeser, R., Christian, S., Finkenzeller, G., Stark, G. B., Héroult, M., and Augustin, H. G. (2008) Spheroid-based engineering of a human vasculature in mice. *Nat. Methods* **5**, 439–445
28. Olsson, A. K., Dimberg, A., Kreuger, J., and Claesson-Welsh, L. (2006) VEGF receptor signalling - in control of vascular function. *Nat. Rev. Mol. Cell Biol.* **7**, 359–371

29. Keskin, U., Totan, Y., Karadağ, R., Erdurmuş, M., and Aydın, B. (2012) Inhibitory effects of SU5416, a selective vascular endothelial growth factor receptor tyrosine kinase inhibitor, on experimental corneal neovascularization. *Ophthalmic Res.* **47**, 13–18
30. Mendel, D. B., Laird, A. D., Smolich, B. D., Blake, R. A., Liang, C., Hannah, A. L., Shaheen, R. M., Ellis, L. M., Weitman, S., Shawver, L. K., and Cherrington, J. M. (2000) Development of SU5416, a selective small molecule inhibitor of VEGF receptor tyrosine kinase activity, as an anti-angiogenesis agent. *Anticancer Drug Des.* **15**, 29–41
31. Fong, T. A., Shawver, L. K., Sun, L., Tang, C., App, H., Powell, T. J., Kim, Y. H., Schreck, R., Wang, X., Risau, W., Ullrich, A., Hirth, K. P., and McMahon, G. (1999) SU5416 is a potent and selective inhibitor of the vascular endothelial growth factor receptor (Flk-1/KDR) that inhibits tyrosine kinase catalysis, tumor vascularization, and growth of multiple tumor types. *Cancer Res.* **59**, 99–106
32. Wilson, I. A., Haft, D. H., Getzoff, E. D., Tainer, J. A., Lerner, R. A., and Brenner, S. (1985) Identical short peptide sequences in unrelated proteins can have different conformations: a testing ground for theories of immune recognition. *Proc. Natl. Acad. Sci. USA* **82**, 5255–5259
33. Ray, B. N., Lee, N. Y., How, T., and Blobe, G. C. (2010) ALK5 phosphorylation of the endoglin cytoplasmic domain regulates Smad1/5/8 signaling and endothelial cell migration. *Carcinogenesis* **31**, 435–441
34. Sawamiphak, S., Seidel, S., Essmann, C. L., Wilkinson, G. A., Pitulescu, M. E., Acker, T., and Acker-Palmer, A. (2010) Ephrin-B2 regulates VEGFR2 function in developmental and tumour angiogenesis. *Nature* **465**, 487–491
35. Lanahan, A. A., Hermans, K., Claes, F., Kerley-Hamilton, J. S., Zhuang, Z. W., Giordano, F. J., Carmeliet, P., and Simons, M. (2010) VEGF receptor 2 endocytic trafficking regulates arterial morphogenesis. *Dev. Cell* **18**, 713–724
36. Bruns, A. F., Herbert, S. P., Odell, A. F., Jopling, H. M., Hooper, N. M., Zachary, I. C., Walker, J. H., and Ponnambalam, S. (2010) Ligand-stimulated VEGFR2 signaling is regulated by co-ordinated trafficking and proteolysis. *Traffic* **11**, 161–174
37. Rosen, L. S., Hurwitz, H. I., Wong, M. K., Goldman, J., Mendelson, D. S., Figg, W. D., Spencer, S., Adams, B. J., Alvarez, D., Seon, B. K., Theuer, C. P., Leigh, B. R., and Gordon, M. S. (2012) A phase I first-in-human study of TRC105 (anti-endoglin antibody) in patients with advanced cancer. *Clin. Cancer Res.* **18**, 4820–4829
38. Karzai, F. H., Apolo, A. B., Cao, L., Madan, R. A., Adelberg, D. E., Parnes, H., McLeod, D. G., Harold, N., Peer, C., Yu, Y., Tomita, Y., Lee, M. J., Lee, S., Trepel, J. B., Gulley, J. L., Figg, W. D., and Dahut, W. L. (2015) A phase I study of TRC105 anti-endoglin (CD105) antibody in metastatic castration-resistant prostate cancer. *BJU Int.* **116**, 546–555
39. Duffy, A. G., Ulahannan, S. V., Cao, L., Rahma, O. E., Makarova-Rusher, O. V., Kleiner, D. E., Fioravanti, S., Walker, M., Carey, S., Yu, Y., Venkatesan, A. M., Turkbey, B., Choyke, P., Trepel, J., Bollen, K. C., Steinberg, S. M., Figg, W. D., and Greten, T. F. (2015) A phase II study of TRC105 in patients with hepatocellular carcinoma who have progressed on sorafenib. *United European Gastroenterol. J.* **3**, 453–461
40. Apolo, A. B., Karzai, F. H., Trepel, J. B., Alarcon, S., Lee, S., Lee, M. J., Tomita, Y., Cao, L., Yu, Y., Merino, M. J., Madan, R. A., Parnes, H. L., Steinberg, S. M., Rodriguez, B. W., Seon, B. K., Gulley, J. L., Arlen, P. M., Dawson, N. A., Figg, W. D., and Dahut, W. L. (2017) A phase II clinical trial of TRC105 (anti-endoglin antibody) in adults with advanced/metastatic urothelial carcinoma. *Clin. Genitourin Cancer)* **15**, 77–85
41. Lebrin, F., Goumans, M. J., Jonker, L., Carvalho, R. L., Valdimarsdottir, G., Thorikay, M., Mummery, C., Arthur, H. M., and ten Dijke, P. (2004) Endoglin promotes endothelial cell proliferation and TGF-beta/ALK1 signal transduction. *EMBO J.* **23**, 4018–4028
42. Ardelean, D. S., Jerkic, M., Yin, M., Peter, M., Ngan, B., Kerbel, R. S., Foster, F. S., and Letarte, M. (2014) Endoglin and activin receptor-like kinase 1 heterozygous mice have a distinct pulmonary and hepatic angiogenic profile and response to anti-VEGF treatment. *Angiogenesis* **17**, 129–146
43. Koleva, R. I., Conley, B. A., Romero, D., Riley, K. S., Marto, J. A., Lux, A., and Vary, C. P. (2006) Endoglin structure and function: determinants of endoglin phosphorylation by transforming growth factor-beta receptors. *J. Biol. Chem.* **281**, 25110–25123
44. Larrivée, B., Prahst, C., Gordon, E., del Toro, R., Mathivet, T., Duarte, A., Simons, M., and Eichmann, A. (2012) ALK1 signaling inhibits angiogenesis by cooperating with the Notch pathway. *Dev. Cell* **22**, 489–500
45. Ricard, N., Ciais, D., Levet, S., Subileau, M., Mallet, C., Zimmers, T. A., Lee, S. J., Bidart, M., Feige, J. J., and Bailly, S. (2012) BMP9 and BMP10 are critical for postnatal retinal vascular remodeling. *Blood* **119**, 6162–6171
46. Lee, N. Y., Golzio, C., Gatza, C. E., Sharma, A., Katsanis, N., and Blobe, G. C. (2012) Endoglin regulates PI3-kinase/Akt trafficking and signaling to alter endothelial capillary stability during angiogenesis. *Mol. Biol. Cell* **23**, 2412–2423
47. Ballmer-Hofer, K., Andersson, A. E., Ratcliffe, L. E., and Berger, P. (2011) Neuropilin-1 promotes VEGFR-2 trafficking through Rab11 vesicles thereby specifying signal output. *Blood* **118**, 816–826
48. Mahmoud, M., Allinson, K. R., Zhai, Z., Oakenfull, R., Ghandi, P., Adams, R. H., Fruttiger, M., and Arthur, H. M. (2010) Pathogenesis of arteriovenous malformations in the absence of endoglin. *Circ. Res.* **106**, 1425–1433
49. Simonds, J., Miller, F., Mandel, J., and Davidson, T. M. (2009) The effect of bevacizumab (Avastin) treatment on epistaxis in hereditary hemorrhagic telangiectasia. *Laryngoscope* **119**, 988–992
50. Deng, T., Zhang, L., Liu, X. J., Xu, J. M., Bai, Y. X., Wang, Y., Han, Y., Li, Y. H., and Ba, Y. (2013) Bevacizumab plus irinotecan, 5-fluorouracil, and leucovorin (FOLFIRI) as the second-line therapy for patients with metastatic colorectal cancer, a multicenter study. *Med. Oncol.* **30**, 752
51. TARGET Study Group. (2007) Sorafenib in advanced clear-cell renal-cell carcinoma. *N. Engl. J. Med.* **356**, 125–134
52. Motzer, R. J., Hutson, T. E., Tomczak, P., Michaelson, M. D., Bukowski, R. M., Rixe, O., Oudard, S., Negrier, S., Szczylik, C., Kim, S. T., Chen, I., Bycott, P. W., Baum, C. M., and Figlin, R. A. (2007) Sunitinib versus interferon alfa in metastatic renal-cell carcinoma. *N. Engl. J. Med.* **356**, 115–124
53. Dorff, T. B., Longmate, J. A., Pal, S. K., Stadler, W. M., Fishman, M. N., Vaishampayan, U. N., Rao, A., Pinksi, J. K., Hu, J. S., Quinn, D. I., and Lara, P. N. Jr. (2017) Bevacizumab alone or in combination with TRC105 for patients with refractory metastatic renal cell cancer. *Cancer* **123**, 4566–4573
54. Anderberg, C., Cunha, S. I., Zhai, Z., Cortez, E., Pardali, E., Johnson, J. R., Franco, M., Páez-Ribes, M., Cordiner, R., Fuxe, J., Johansson, B. R., Goumans, M. J., Casanovas, O., ten Dijke, P., Arthur, H. M., and Pietras, K. (2013) Deficiency for endoglin in tumor vasculature weakens the endothelial barrier to metastatic dissemination. *J. Exp. Med.* **210**, 563–579
55. Paauwe, M., Heijkants, R. C., Oudt, C. H., van Pelt, G. W., Cui, C., Theuer, C. P., Hardwick, J. C., Sier, C. F., and Hawinkels, L. J. (2016) Endoglin targeting inhibits tumor angiogenesis and metastatic spread in breast cancer. *Oncogene* **35**, 4069–4079
56. Yee, K. W., O'Farrell, A. M., Smolich, B. D., Cherrington, J. M., McMahon, G., Wait, C. L., McGreevey, L. S., Griffith, D. J., and Heinrich, M. C. (2002) SU5416 and SU5614 inhibit kinase activity of wild-type and mutant FLT3 receptor tyrosine kinase. *Blood* **100**, 2941–2949
57. Smolich, B. D., Yuen, H. A., West, K. A., Giles, F. J., Albitar, M., and Cherrington, J. M. (2001) The antiangiogenic protein kinase inhibitors SU5416 and SU6668 inhibit the SCF receptor (c-kit) in a human myeloid leukemia cell line and in acute myeloid leukemia blasts. *Blood* **97**, 1413–1421
58. Gordon, M. S., Robert, F., Matei, D., Mendelson, D. S., Goldman, J. W., Chiorean, E. G., Strother, R. M., Seon, B. K., Figg, W. D., Peer, C. J., Alvarez, D., Adams, B. J., Theuer, C. P., and Rosen, L. S. (2014) An open-label phase Ib dose-escalation study of TRC105 (anti-endoglin antibody) with bevacizumab in patients with advanced cancer. *Clin. Cancer Res.* **20**, 5918–5926

Received for publication August 21, 2017.
Accepted for publication December 26, 2017.